elongation (one family) of the coded proteins (Table 3). In a family with a 32,787 nucleotides deletion (the exact deletion size was determined in Daniel Bichet's lab in Montreal), two affected brothers showed complete NDI. Their mother and sister were asymptomatic heterozygous carriers of the mutation. In another family having a large deletion (4,586 nucleotides), a boy was affected with complete NDI and his mother was a heterozygous carrier. A 1-nucleotide deletion was observed in a complete NDI boy, and his mother was a heterozygous carrier of the mutation. In two families having 2-nucleotide or 14-nucleotide deletion mutations, the index patients were females who were diagnosed as having complete NDI after stimulation tests.

Three novel small (1–2 nucleotides) frame-shift insertion mutations were found in three families in which the index patients were males with complete NDI. All of these mutations are expected to introduce a premature stop codon, and the mutations were conserved within the families (Table 3).

Frequency of symptomatic carriers of AVPR2 mutations

Carriers of disease-causing mutations of AVPR2 (females having heterozygous mutations) sometimes manifest NDI symptoms [22, 23]; however, it is unknown how often this event occurs. In our present study, in 52 NDI families with AVPR2 mutations, at least one female member (usually a mother of an affected boy) were genetically analyzed and found to have the disease-causing allele. In a total of 64 such female subjects, 16 (25 %) had symptoms of polyuria and polydipsia, while 43 (67 %) were asymptomatic. Among the 16 symptomatic female subjects, 4 were diagnosed as having complete NDI, and 3 were the probands in each family. The types of mutations identified in these symptomatic carriers were: missense mutations (8), deletion mutations (6), nonsense mutation (1), and insertion mutation (1), indicating that this event occurs in any type of mutation.

The mechanism for the appearance of NDI symptoms in female carriers is explained by an extremely skewed inactivation of the normal allele of the X chromosome [24]; the frequency of this event was estimated to be very rare [9]. However, a recent study by Sato et al. [25] showed that a moderately skewed inactivation of the normal allele is enough to cause NDI symptoms. This result implies that symptomatic female carriers occur more often than previously thought. Our data are consistent with this speculation, and show that one fourth of carriers of AVPR2 disease-causing mutations present NDI symptoms. Thus, female patients with NDI symptoms require a careful examination, and gene mutation analysis for AVPR2 should be considered if other causes are unlikely.
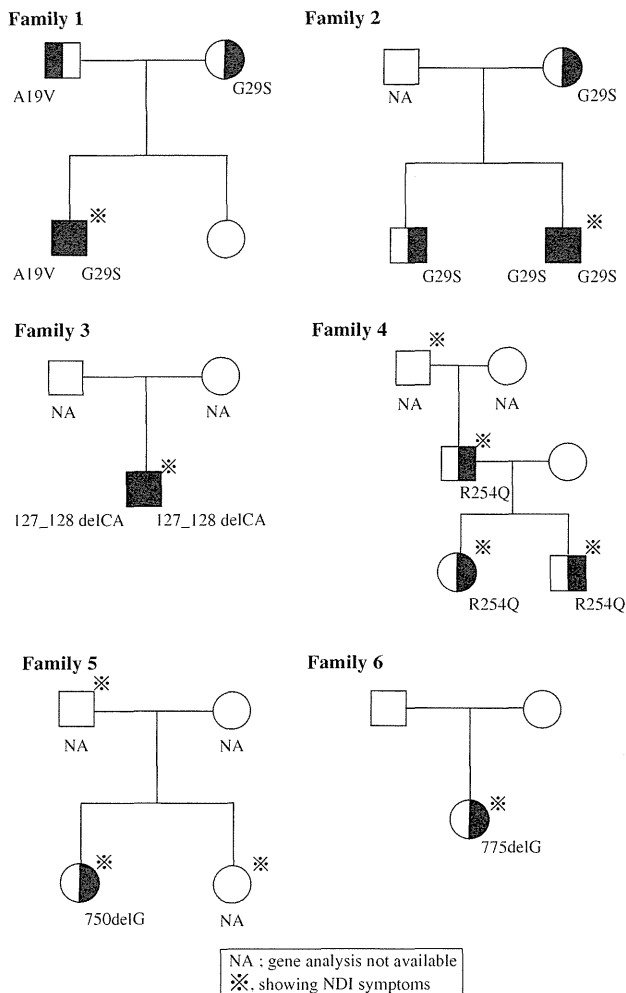
AQP2 mutations causing NDI

Nine AQP2 mutations were identified in 9 NDI families (Table 4). The results from 3 of these families were previously reported [12]. These three families had monoallelic frame-shift deletion mutations (1–10 nucleotides) in the C-terminus of AQP2 (different mutations in each family), and showed an autosomal dominant inheritance with a slightly milder form of NDI [12]. The remaining six families were newly analyzed in the present study, and 6 different NDI-causing mutations were found (Table 4). These mutations consisted of 3 missense mutations and 3 deletion mutations (1–2 nucleotides deletions); 3 of them were novel mutations, and other three were recurrences of previously known mutations. Two missense mutations and one deletion mutation showed a recessive inheritance mode, while one missense mutation and two small deletion mutations manifested a dominant inheritance mode.

The family trees and results of mutation analysis of newly analyzed families are summarized in Fig. 1. In family 1, two missense mutations (A19V and G29S) were compound heterozygous in a male NDI patient and manifested by vasopressin-unresponsive polyuria (8–10 L/day). The patient's parents were asymptomatic. The father carried a novel A19V mutation, while the mother had a G29S mutation, which was previously reported to be causative [26]. In family 2, the G29S mutation (the same one found in family 1) was homozygous in the proband,

Table 4 Disease-causing *AQP2* mutations

Nucleotide change	Amino acid change	Inheritance mode	References
Newly analyzed			
Missense mutations			
c.56C>T	A19V	Recessive	New
c.85G>A	G29S	Recessive	Sahakitrungruang et al. [26]
c.761G>A	R254Q	Dominant	Savelkoul et al. [28]
Deletion mutations			
c.127_128delCA	FS/105X	Recessive	Tajima et al. [27]
c.750delG	FS/334X	Dominant	New
c.775delC	FS/334X	Dominant	New
Previously analyzed			
Deletion mutations			
c.721delG	FS/334X	Dominant	Kuwahara et al. [12]
c.763–772del	FS/331X	Dominant	Kuwahara et al. [12]
c.812–818del	FS/332X	Dominant	Kuwahara et al. [12]

Family 1 A19V G29S A19V G29S ※

Family 2 NA G29S G29S G29S G29S ※

Family 3 NA NA 127_128 delCA 127_128 delCA ※

Family 4 ※ NA NA R254Q ※ R254Q ※ R254Q ※

Family 5 ※ NA NA 750delG ※ NA ※

Family 6 775delG ※

NA : gene analysis not available
※ : showing NDI symptoms

Fig. 1 AOP2 mutations newly found in Japanese NDI families. Six different AQP2 mutations were found in six Japanese NDI families. *NA* gene analysis not available. *Showing NDI symptoms

relatives had NDI symptoms, but have not been clinically examined. The siblings (a 1-year-old boy and a 3-year-old girl) showed similar clinical characteristics of polyuria and polydipsia starting 4–6 months after birth, and slight responsiveness of urine osmolality to vasopressin (maximum urine osmolality was about 500 mOsm/L after vasopressin administration). Consistent with these observation, this mutation (R254Q) was recently reported as an NDI causative mutation with dominant inheritance [28]. Another missense mutation on this residue, R254L, was also reported to cause a similar NDI phenotype [29]. In the heterologous expression studies, the R254Q-AQP2 protein was impaired in its AVP-elicited phosphorylation of Ser256, which is a key step for AQP2 trafficking to the apical membrane [28]. The dominant inheritance can be explained by hetero-oligomerization of wild-type/mutant AQP2 proteins and dominant-negative effect of mutant protein on wild-type protein [7].

In a female patient of family 5, a novel heterozygous 1-nucleotide deletion mutation (750delG) was found. The patient's sister and father were symptomatic. Her urine osmolality did not respond to vasopressin. This mutation causes a frame shift, with a new amino acids sequence starting from Val251 and ending at codon 334 in the C-terminal of AQP2. In Family 6, a 2-year-old girl was found to have a novel heterozygous 1-nucleotide deletion mutation (775delC) that causes frame shift with a new C-terminus starting at Leu259. The parents did not show NDI symptoms and did not carry the mutation, which indicated that the mutation occurred de novo. The girl showed polyuria and polydipsia and NDI was diagnosed by water deprivation and vasopressin administration tests. These identified two deletion mutations cause frame shifts from Val251 and Leu259 and a new C-terminal tail ending at codon 334 (Table 4). We previously reported three small deletion mutations in the C-terminus that cause similar frame shifts and show dominant inheritance [12] (Table 4). These frame-shift mutations share the loss of the last tail of the AQP2 protein, the site where PDZ proteins and ubiquitines interact, and the presence of extended C-terminal tails that contain missorting signals. As a result of these effects, these mutant AQP2 proteins making tetramers with wild-type proteins are incorrectly translocated to the basolateral membrane instead of the apical membrane [20, 30, 31]. This missorting is confirmed in knockin mice harboring a human C-terminal deletion mutation (c.763–772del) [32]. It is interesting that these deletion mutations are observed more often that missense mutations in Japanese patients, which is different from the frequencies in a total global summary [3, 20].

We could not detect mutations in the two genes in seven families (9 %, Table 1). It is said that causative gene mutations cannot be found in approximately 5 % of all

and his healthy mother and brother were heterozygous for the mutation. The patient exhibited polyuria (urine volume was 10–15 L/day), and the urine osmolality did not respond to vasopressin (maximum urine osmolality was about 100 mOsm/L). The appearance of NDI symptoms only when the mutations are compound heterozygous or homozygous strongly indicates that these two missense mutations are disease causative.

In family 3, a homozygous 2-nucleotide deletion mutation (c.127_128delCA) was found in a neonatal boy who exhibited polyuria and dehydration. His urine osmolality did not respond to vasopressin (< 150 mOsm/L). The resultant frame shift predicts new amino acids starting at codon 43, with a premature stop at codon 105. The same mutation was found in an unrelated Japanese family and has been reported by others [27].

In family 4, a monoallelic R254Q mutation was found in two siblings and their father. The father and paternal

congenital NDI patients [4]. Possibilities such as the presence of mutations in the promoter regions of the AVPR2 or AQP2 genes are a likely explanation [4]. Our mutational analysis does not usually cover the promoter regions; thus, this possibility remains to be examined. To date, no genes other than AVPR2 and AQP2 have been attributed to NDI. However, it is possible that mutations in the genes encoding signaling cascade molecules connecting these two key membrane proteins cause NDI. Progress in gene mutational analysis methods such as whole-exome sequencing will address this possibility.
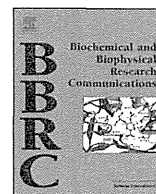
References

1. Morello JP, Bichet DG. Nephrogenic diabetes insipidus. Annu Rev Physiol. 2001;63:607–30.
2. Sasaki S. Nephrogenic diabetes insipidus: update of genetic and clinical aspects. Nephrol Dial Transpl. 2004;19:1351–3.
3. Babey M, Kopp P, Robertson GL. Familial forms of diabetes insipidus: clinical and molecular characteristics. Nat Rev Endocrinol. 2011;7:701–14.
4. Wesche D, Deen PM, Knoers NV. Congenital nephrogenic diabetes insipidus: the current state of affairs. Pediatr Nephrol. 2012. PubMed PMID: 22427315.
5. Birnbaumer M, Seibold A, Gilbert S, Ishido M, Barberis C, Antaramian A, et al. Molecular cloning of the receptor for human antidiuretic hormone. Nature. 1992;357:333–5.
6. Fushimi K, Uchida S, Hara Y, Hirata Y, Marumo F, Sasaki S. Cloning and expression of apical membrane water channel of rat kidney collecting tubule. Nature. 1993;361:549–52.
7. Loonen AJ, Knoers NV, van Os CH, Deen PM. Aquaporin 2 mutations in nephrogenic diabetes insipidus. Semin Nephrol. 2008;28:252–65.
8. Noda Y, Sohara E, Ohta E, Sasaki S. Aquaporins in kidney pathophysiology. Nat Rev Nephrol. 2010;6:168–78.
9. Sasaki S, Fushimi K, Saito H, Saito F, Uchida S, Ishibashi K, et al. Cloning, characterization, and chromosomal mapping of human aquaporin of collecting duct. J Clin Invest. 1994;93:1250–6.
10. Deen PM, Verdijk MA, Knoers NV, Wieringa B, Monnens LA, van Os CH, et al. Requirement of human renal water channel aquaporin-2 for vasopressin-dependent concentration of urine. Science. 1994;264:92–5.
11. Arthus MF, Lonergan M, Crumley MJ, Naumova AK, Morin D, De Marco LA, et al. Report of 33 novel AVPR2 mutations and analysis of 117 families with X-linked nephrogenic diabetes insipidus. J Am Soc Nephrol. 2000;11:1044–54.
12. Kuwahara M, Iwai K, Ooeda T, Igarashi T, Ogawa E, Katsushima Y, et al. Three families with autosomal dominant nephrogenic diabetes insipidus caused by aquaporin-2 mutations in the C-terminus. Am J Hum Genet. 2001;69:738–48.
13. Owada M, Kawamura M, Kimura Y, Fujiwara T, Uchida S, Sasaki S, et al. Water intake and 24-hour blood pressure monitoring in a patient with nephrogenic diabetes insipidus caused by a novel mutation of the vasopressin V2R gene. Intern Med. 2002; 41:119–23.
14. Mizuno H, Sugiyama Y, Ohro Y, Imamine H, Kobayashi M, Sasaki S, et al. Clinical characteristics of eight patients with congenital nephrogenic diabetes insipidus. Endocrine. 2004;24: 55–9.
15. Ashida A, Yamamoto D, Nakakura H, Matsumura H, Uchida S, Sasaki S, et al. A case of nephrogenic diabetes insipidus with a novel missense mutation in the AVPR2 gene. Pediatr Nephrol. 2007;22:670–3.
16. Fujimoto M, Imai K, Hirata K, Kashiwagi R, Morinishi Y, Kitazawa K, et al. Immunological profile in a family with nephrogenic diabetes insipidus with a novel 11 kb deletion in AVPR2 and ARHGAP4 genes. BMC Med Genet. 2008;9:42.
17. Bichet DG, Birnbaumer M, Lonergan M, Arthus MF, Rosenthal W, Goodyer P, et al. Nature and recurrence of AVPR2 mutations in X-linked nephrogenic diabetes insipidus. Am J Hum Genet. 1994;55:278–86.
18. Bichet DG, Arthus MF, Lonergan M, Hendy GN, Paradis AJ, Fujiwara TM, et al. X-linked nephrogenic diabetes insipidus mutations in North America and the Hopewell hypothesis. J Clin Invest. 1993;92:1262–8.
19. Spanakis E, Milord E, Gragnoli C. AVPR2 variants and mutations in nephrogenic diabetes insipidus: review and missense mutation significance. J Cell Physiol. 2008;217:605–17.
20. Sasaki S. Aquaporin 2: from its discovery to molecular structure and medical implications. Mol Asp Med. 2012;33:535–46.
21. Faerch M, Christensen JH, Corydon TJ, Kamperis K, de Zegher F, Gregersen N, et al. Partial nephrogenic diabetes insipidus caused by a novel mutation in the AVPR2 gene. Clin Endocrinol (Oxf). 2008;68:395–403.
22. Moses AM, Sangani G, Miller JL. Proposed cause of marked vasopressin resistance in a female with an X-linked recessive V2 receptor abnormality. J Clin Endocrinol Metab. 1995;80:1184–6.
23. van Lieburg AF, Verdijk MA, Schoute F, Ligtenberg MJ, van Oost BA, Waldhauser F, et al. Clinical phenotype of nephrogenic diabetes insipidus in females heterozygous for a vasopressin type 2 receptor mutation. Hum Genet. 1995;96:70–8.
24. Nomura Y, Onigata K, Nagashima T, Yutani S, Mochizuki H, Nagashima K, et al. Detection of skewed X-inactivation in two female carriers of vasopressin type 2 receptor gene mutation. J Clin Endocrinol Metab. 1997;82:3434–7.
25. Satoh M, Ogikubo S, Yoshizawa-Ogasawara A. Correlation between clinical phenotypes and X-inactivation patterns in six female carriers with heterozygote vasopressin type 2 receptor gene mutations. Endocr J. 2008;55:277–84.
26. Sahakitrungruang T, Wacharasindhu S, Sinthuwiwat T, Supornsilchai V, Suphapeetiporn K, Shotelersuk V. Identification of two novel aquaporin-2 mutations in a Thai girl with congenital nephrogenic diabetes insipidus. Endocrine. 2008;33:210–4.
27. Tajima T, Okuhara K, Satoh K, Nakae J, Fujieda K. Two novel aquaporin-2 mutations in a sporadic Japanese patient with autosomal recessive nephrogenic diabetes insipidus. Endocr J. 2003; 50:473–6.
28. Savelkoul PJ, De Mattia F, Li Y, Kamsteeg EJ, Konings IB, van der Sluijs P, et al. p.R254Q mutation in the aquaporin-2 water channel causing dominant nephrogenic diabetes insipidus is due

to a lack of arginine vasopressin-induced phosphorylation. Hum Mutat. 2009;30:E891–903.

29. de Mattia F, Savelkoul PJ, Kamsteeg EJ, Konings IB, van der Sluijs P, Mallmann R, et al. Lack of arginine vasopressin-induced phosphorylation of aquaporin-2 mutant AQP2-R254L explains dominant nephrogenic diabetes insipidus. J Am Soc Nephrol. 2005;16:2872–80.

30. Asai T, Kuwahara M, Kurihara H, Sakai T, Terada Y, Marumo F, et al. Pathogenesis of nephrogenic diabetes insipidus by aquaporin-2 C-terminus mutations. Kidney Int. 2003;64:2–10.

31. Kamsteeg EJ, Bichet DG, Konings IB, Nivet H, Lonergan M, Arthus MF, et al. Reversed polarized delivery of an aquaporin-2 mutant causes dominant nephrogenic diabetes insipidus. J Cell Biol. 2003;163:1099–109.

32. Sohara E, Rai T, Yang SS, Uchida K, Nitta K, Horita S, et al. Pathogenesis and treatment of autosomal-dominant nephrogenic diabetes insipidus caused by an aquaporin 2 mutation. Proc Natl Acad Sci USA. 2006;103:14217–22.

Contents lists available at SciVerse ScienceDirect

Biochemical and Biophysical Research Communications

KLHL2 interacts with and ubiquitinates WNK kinases

Daiei Takahashi, Takayasu Mori, Mai Wakabayashi, Yutaro Mori, Koichiro Susa, Moko Zeniya, Eisei Sohara, Tatemitsu Rai, Sei Sasaki, Shinichi Uchida *

Department of Nephrology, Graduate School of Medical and Dental Sciences, Tokyo Medical and Dental University, Japan

ABSTRACT

Mutations in the WNK1 and WNK4 genes result in an inherited hypertensive disease, pseudohypoaldosteronism type II (PHAII). Recently, the KLHL3 and Cullin3 genes were also identified as responsible genes for PHAII. Although we have reported that WNK4 is a substrate for the KLHL3–Cullin3 E3 ligase complex, it is not clear whether all of the WNK isoforms are regulated only by KLHL3. To explore the interaction of WNKs and other Kelch-like proteins, we focused on KLHL2 (Mayven), a human homolog of *Drosophila* Kelch that shares the highest similarity with KLHL3. We found that KLHL2, as well as KLHL3, was co-immunoprecipitated with all four WNK isoforms. The direct interaction of KLHL2 with WNKs was confirmed on fluorescence correlation spectroscopy. Co-expression of KLHL2 and Cullin3 decreased the abundance of WNK1, WNK3 and WNK4 within HEK293T cells, and a significant increase of WNK4 ubiquitination by KLHL2 and Cullin3 was observed both in HEK293T cells and in an in vitro ubiquitination assay. These results suggest that KLHL2–Cullin3 also functions as an E3-ligase for WNK isoforms within the body.

© 2013 Elsevier Inc. All rights reserved.

1. Introduction

Mutations in the with-no-lysine kinase 1 (WNK1) and WNK4 genes are responsible for pseudohypoaldosteronism type II (PHAII) [1], which is characterized by hypertension, hyperkalemia, and metabolic acidosis [2]. Numerous studies have been performed to clarify the molecular pathogenesis of PHAII [3]. We have found that increased phosphorylation of oxidative stress-responsive kinase 1 (OSR1) and STE20/SPS1-related proline/alanine-rich kinase (SPAK), which are substrates of WNK kinases, results in the activation of the Na-Cl cotransporter (NCC) in vivo [4–6]. The analysis of WNK4$^{-/-}$ mice was concordant with our hypothesis that WNK4 kinase is a major regulator of NCC phosphorylation in kidney [7].

In 2011, additional genes responsible for PHAII (KLHL3 and Cullin3) were identified [8,9]. KLHL3 is a member of the BTB-Kelch protein family, which includes components of the Cullin-RING E3 ubiquitin ligases and a substrate adaptor for ubiquitination [10–12]. Recently, we reported that KLHL3 interacted with Cullin3 and WNK4, induced WNK4 ubiquitination, and reduced WNK4 protein abundance. We also revealed the pathophysiological role of PHAII-causing mutations of the WNK4, KLHL3 and Cullin3 genes [13]. Namely, the mutations caused impaired ubiquitination and a subsequent increase of WNK4 in the kidney, which activate the WNK-OSR1/SPAK-NCC signal cascade and cause PHAII [13]. Two independent reports have supported our findings [14,15]. In

addition to WNK4, Alessi's group reported that WNK1 interacts with the KLHL3–Cullin3 complex in vitro [16]. This data is quite reasonable since we identified that the domain within WNK4 responsible for the binding to KLHL3 is an acidic domain that is highly conserved among WNK kinases [13]. Therefore, it would be possible that WNK2 and WNK3 could also be targets of KLHL3–Cullin3 E3 ligase. However, WNK isoforms are widely expressed in various cell types within the body, whereas KLHL3 expression might be relatively limited in specific cell types. In this respect, we hypothesized that there may be other ubiquitin ligases for WNK kinases. Here, we focused on KLHL2 (Mayven), another human homolog of *Drosophila* Kelch, since the Kelch domain (WNK-binding domain) of KLHL2 is highly similar (86% identity) to that of KLHL3. Initially, KLHL2 was identified as an actin-binding protein predominantly expressed in brain [17]. Later, it was found that KLHL2 formed a complex with Cullin3 and bound to and increased the ubiquitination of neuronal pentraxin with chromo domain (NPCD), suggesting its role as E3 ubiquitin ligase [18]. In the present study, we report that KLHL2 binds to WNKs at their acidic domain and functions as an E3 ubiquitin ligase for WNK kinases.

2. Materials and methods

2.1. Plasmids

Expression plasmids for 3xFLAG-tagged human WNK1, WNK4, Cullin3, Halo-tagged human WNK4 and KLHL3 have been described previously [13,19,20]. The cDNA encoding Halo-tagged

---

* Corresponding author. Address: 1-5-45 Yushima, Bunkyo, Tokyo 113-8519, Japan. Fax: +81 3 5803 5215.
   E-mail address: suchida.kid@tmd.ac.jp (S. Uchida).

human WNK1, WNK2, WNK3 and GAPDH in pFN21A vector were purchased from Promega. Human KLHL2 cDNA was isolated by reverse transcription-polymerase chain reaction using human brain mRNA from human total RNA master panel II (Clontech) as a template. Sequence of the amplification primers employed is as follows: KLHL2 sense, 5′-ATC GAT CGA TAT GGA GAC GCC GCC GCT GCC-3′; KLHL2 antisense, 5′-CCG GCG CGC CGT TTA AAC TCA TAA TGG TTT ATC AAT AAC-3′. The cDNA was cloned into pFN21A vector (Promega). HA$_4$-tagged ubiquitin expression vector was kindly provided by T. Ohta (St. Marianna University, School of Medicine).

2.2. Reverse transcription polymerase chain reaction

RNAs from human total RNA master panel II (Clontech) were reverse-transcribed by using Omniscript RT kit (QIAGEN). The target cDNAs were amplified by PCR, which was performed by using primers described below. The primers for GAPDH were purchased from Roche Diagnostics. Sequence of the amplification primers employed is as follows: KLHL2 sense, 5′-TAA TAC CGA AAA ACA CTG CC-3′; KLHL2 antisense, 5′-TTC TAA CTC TCT TTG CTC GG-3′; KLHL3 sense, 5′-TGA CAA GAA CCA GAG GAC GA-3′; KLHL3 antisense, 5′-AAC TGA GAC TGC AGG AAG-3′.

2.3. Cell culture and transfections

HEK293T cells were cultured in Dulbecco's modified Eagle's medium (DMEM) supplemented with 10% (v/v) fetal bovine serum (FBS), 2 mM L-glutamine, 100 U/ml penicillin, and 0.1 mg/ml streptomycin at 37 °C in a humidified 5% CO$_2$ incubator. HEK293T cells (3 × 10^5 cells/6-cm dish) were transfected by the indicated amount of plasmid DNA with Lipofectamine 2000 reagent (Invitrogen).

2.4. Immunoprecipitation

HEK293T cells transfected with the indicated amount of DNA were lysed in a buffer (50 mM Tris–HCl (pH 7.5), 150 mM NaCl, 1% Nonidet P-40, 1 mM sodium orthovanadate, 50 mM sodium fluoride, and protease inhibitor cocktail) for 30 min at 4 °C. When the cells were transfected with the HA-ubiquitin expression plasmid, the cells were treated with 1 μM epoxomicin (specific and irreversible proteasome inhibitor; Peptide Institute, Osaka, Japan) for 3 h before harvesting. After centrifugation at 12,000×g for 15 min, the protein concentration of the supernatants was measured and equal amounts of the supernatants were used for immunoprecipitation with anti-FLAG M2 beads (Sigma–Aldrich) for 1 h at 4 °C. Thereafter, the precipitants were washed with the lysis buffer and the immunoprecipitates were eluted in SDS sample buffer after boiling for 5 min. To detect ubiquitination of WNK4 in denatured samples, the cells transfected with various plasmids were lysed in 2% SDS buffer (2% SDS, 150 mM NaCl, 10 mM Tris–HCl, pH 8.0, 2 mM sodium orthovanadate, 50 mM sodium fluoride, 1× protease inhibitors) and boiled for 10 min followed by sonication. Before immunoprecipitation, the lysates were diluted 1:10 in a dilution buffer (10 mM Tris–HCl, pH 8.0, 150 mM NaCl, 2 mM EDTA, 1% Triton X-100), incubated at 4 °C for 1 h with rotation, and centrifuged at 12,000×g for 15 min.

2.5. Immunoblotting

Cells transfected with the indicated amount of plasmid DNA were lysed in lysis buffer [50 mM Tris–HCl, pH 7.5, 150 mM NaCl, 1% Nonidet P-40, 1 mM sodium orthovanadate, 50 mM sodium fluoride, and protease inhibitor cocktail (Roche Diagnostics)] for 30 min at 4 °C. After centrifugation at 12,000×g for 15 min, the supernatants were boiled with SDS sample-buffer (Cosmo Bio,

Inc.) and subjected to SDS–PAGE. Blots were probed with the following primary antibodies: anti-FLAG (Sigma–Aldrich), anti-Halo (Promega), anti-HA (Merck Millipore), anti-T7 (Merck Millipore) and anti-actin (Cytoskelton) antibodies. Alkaline-phosphatase-conjugated anti-IgG antibodies (Promega, Madison, WI) and WesternBlue (Promega) were used to detect the signals.

2.6. In vitro ubiquitination assay

GST-WNK4(490–626) in pGEX6p-1 vector was described previously [13]. Recombinant GST-fusion WNK4 protein was expressed in BL21 *Eschericia coli* cells and purified by using glutathione sepharose beads. KLHL2 or KLHL3 complexes were immunoprecipitated from the lysates of HEK293T cells transiently expressing FLAG-KLHL2 or FLAG-KLHL3. Then, the complexes were incubated in a 20 μl volume of reaction buffer (50 mM Tris–HCl, pH 7.4, 2.5 mM MgCl$_2$, 0.5 mM DTT, 2 mM ATP) for 2 h at 30 °C with purified GST-WNK4-His (1 μg), 100 ng recombinant human E1 (Boston Biochem), 500 ng recombinant human UbcH5a/UBE2D1 (Boston Biochem), and 2.5 μg recombinant human ubiquitin (Boston Biochem). The reaction was terminated by addition of SDS–PAGE sample buffer, followed by boiling for 5 min. The reaction mixtures were then subjected to immunoblot analyses with anti Ub (Cell Signaling Technology) or His (Abcam) antibodies.

2.7. Fluorescence correlation spectroscopy

Fluorescent TAMRA-labeled WNK1, 2, 3 and WNK4 peptides covering the PHAII mutation sites were prepared (Hokkaido System Science Co., Ltd., Hokkaido, Japan). Kelch-repeats of human KLHL2 or KLHL3 were cloned into pGEX6P-1 vector. Recombinant GST-fusion KLHL proteins were expressed in BL21 *E. coli* cells and purified by using glutathione sepharose beads. The TAMRA-labeled WNK peptides were incubated at room temperature for 30 min with different concentrations of GST-KLHL proteins (0–2 μM) in 1× PBS with 0.05% Tween 20 reaction buffer and the fluorescence correlation spectroscopy (FCS) measurements of single-molecule fluorescence were performed using the FluoroPoint-light analytical system (Olympus, Tokyo, Japan) [21]. The assay was performed in a 384-well plate. All experiments were performed in 10 s of data acquisition time and the measurements were repeated five times per sample. The amino acid sequence of TAMRA-WNKs is as follows: WNK1, TAMRA-SVSTQVEPEEPEADQHQQLQYQQPSISVLS (30 aa); WNK2, TAMRA-GQPGPPEPEEPEADQHLLPPTLPTSATSLA (30 aa); WNK3, TAMRA-AQQTGAECEETEVDQHVRQQLLQRKPQQHC (30 aa); WNK4, TAMRA-PSVFPPEPEEPEADQHQPFLFRHASYSSTT (30 aa). Acidic domains of each WNK isoform are underlined.

2.8. Statistics

Statistical significance was evaluated by ANOVA test with multiple comparisons using Tukey's correction. The results with *p* values <0.05 were considered statistically significant. Data are presented as mean ± SEM.

3. Results

3.1. Expression pattern of KLHL2 and KLHL3 in human organs

To examine the distribution of KLHL2 and KLHL3 expression, we performed RT-PCR of KLHL2 and KLHL3 cDNA in human organs (Fig. 1). cDNA from the indicated human tissues was used as a template for PCR by using primers specific for KLHL2, KLHL3 and GAPDH mRNA. KLHL2 as well as KLHL3 was expressed differently in various human organs.

3.2. Overexpressed KLHL2 interacts with WNK kinases

We first confirmed the interaction of KLHL2 and Cullin3 by co-immunoprecipitation (Fig. 2A) as previously reported [18]. To investigate whether KLHL2 interacts with WNK kinases in mammalian cells, we then performed co-immunoprecipitation assays of full-length KLHL2 and KLHL3 with WNK kinases. Because the expression level of Halo-tagged WNK1 was low, we used FLAG-tagged WNK1 in co-immunoprecipitation assays (Fig. 2B). Other WNKs were Halo-tagged (Fig. 2C). We found that KLHL3 could interact with WNK2 and WNK3 as well as WNK1 and WNK4 and that KLHL2 could also interact with all WNK kinases. As in the case with KLHL3, KLHL2 was not co-immunoprecipitated with other components of the WNK-OSR1/SPAK-NCC signal cascade, i.e., OSR1, SPAK, and NCC (Fig. S1).

To investigate whether the conserved acidic domains of WNKs could be the common binding sites for KLHL2 and KLHL3, we prepared TAMRA-labeled WNK peptides covering each acidic motif (Fig. 2D), and the binding to the Kelch-repeat of KLHL2 or KLHL3 proteins was assayed in vitro as we described previously [13]. As shown in Fig. 2D, the diffusion time of TAMRA-labeled peptide became slower as the concentration of GST-KLHLs increased, indicating that all WNK peptides could bind to both GST-KLHL2 and GST-KLHL3. GST alone did not affect the diffusion time. It is notable that the WNK3 peptide showed the slowest diffusion time both with KLHL2 and KLHL3. The amino acid sequence of the WNK3 acidic motif (ECEETEVDQH) was different from those of other WNK kinases (EPEEPEADQH) (Fig. 2D), which might be responsible for the difference in diffusion times.

3.3. KLHL2 regulated the abundance of WNK kinases

To determine the effect of KLHL2 on WNK kinases, we overexpressed KLHL2 or KLHL3 plus Cullin3 along with WNK kinases in HEK293T cells. As shown in Fig. 3, co-expression of KLHL2 or KLHL3 with Cullin3 decreased the levels of WNK1, WNK3, and WNK4 proteins as compared to the expression of Cullin3 alone. In contrast to WNK1, 3, and 4, the effect of KLHL2 on WNK2 was not clear, even after repeating the experiments more than three times.

Fig. 1. Expression of KLHL2 and KLHL3 mRNAs in human organs. Complementary DNAs from the indicated human organs were used as a template for PCR using primers specific for KLHL2, KLHL3 and GAPDH mRNA. The expression patterns of KLHL2 and KLHL3 are different.

3.4. KLHL2 increases the ubiquitination of WNK4

To investigate whether KLHL2 ubiquitinates WNK kinases, we first performed an in vitro ubiquitination assay. FLAG-tagged KLHL2 or KLHL3 expressed in HEK293T cells was immunoprecipitated with M2-agarose and mixed with recombinant E1, E2, ubiquitin, and WNK4 protein (residues 490–626). We did not overexpress Cullin3, since we knew from the preliminary experiments that there was a sufficient amount of endogenous Cullin3 in HEK293T cells to perform this assay (data not shown). We confirmed that KLHL2 directly ubiquitinated WNK4 protein (residues 490–626) (Fig. 4A) as KLHL3 did in our previous study. We also confirmed WNK4 ubiquitination in vivo by immunoprecipitation under a denaturing condition. As shown in the ubiquitin (HA) immunoblot (Fig. 4B), the ubiquitination signals appeared as a smeared band over the apparent molecular size of WNK4 (200 kDa). This ubiquitination was increased by co-expression of KLHL2 or KLHL3, although the immunoprecipitated WNK4 was decreased by co-expression. These results clearly indicate that KLHL2 functions as an E3 ubiquitin ligase of WNK4.

4. Discussion

In the present study, we reported the interaction between KLHL2 and WNK kinases that induced the ubiquitination of WNK protein, leading to a reduced level of WNK protein in cells. KLHL2 was initially identified as an actin-binding protein highly expressed in the brain [17], and it was implicated in oligodendrocyte process outgrowth as well as transcriptional regulation of growth-promoting factors in breast cancer cells [22–24]. However, several members of the Kelch-like protein family have been recently described as components of multi-protein complexes known as Cullin-RING E3 ubiquitin ligases (CRLs) [10,11,25]. CRLs are involved in the identification and targeting of proteins for ubiquitination. Kelch-like proteins function as substrate adapters, recruiting proteins destined for ubiquitination into the CRL complex. In line with this notion, neuronal pentraxin with chromo domain (NPCD) was reported to bind to KLHL2, and its ubiquitination was increased by KLHL2 co-expression [18]. However, no direct evidence showing that KLHL2 is an E3 ligase has been demonstrated.

We observed a highly similar function of KLHL2 to that of KLHL3 as an E3 ubiquitin ligase to WNK kinases. KLHL2 is the closest homolog of KLHL3 among the KLHL proteins, and it is also the closest homolog of drosophila Kelch (63% identity). The Kelch repeats among these three proteins are highly conserved. The four β-strands found in each Kelch repeat are named 'a' to 'd'. It is surprising that not only all of the mutated residues reported in PHAII patients [8,9] are conserved between these three Kelch-like proteins, but also that KLHL2 shares almost perfect identity (98% identity) with KLHL3 when focused on its 'b–c' loops and 'd–a' loops, in which most of the PHAII-causing KLHL3 mutations cluster [8,9]. This high identity between KLHL2 and KLHL3 is not seen between KLHL3 and other Kelch-like proteins [26]. The function of each loop of the KLHL3 Kelch repeat has not been evaluated yet, but considering that the 'd–a' loops and 'b–c' loops of Keap1 form the top face of the β-propeller and that this face is the substrate (Nrf2)-binding pocket [27], the extensive shared identity in these domains between KLHL2 and KLHL3 may support the identity of substrate specificity between KLHL2 and KLHL3.

This study clearly shows that not only WNK1 and WNK4 but all WNK kinases could be regulated by KLHL3. In addition, KLHL2 could regulate all WNKs as well. In the case of WNK4, the dysregulation of WNK4 degradation significantly affected the downstream signaling and caused PHAII. In this respect, the regulation
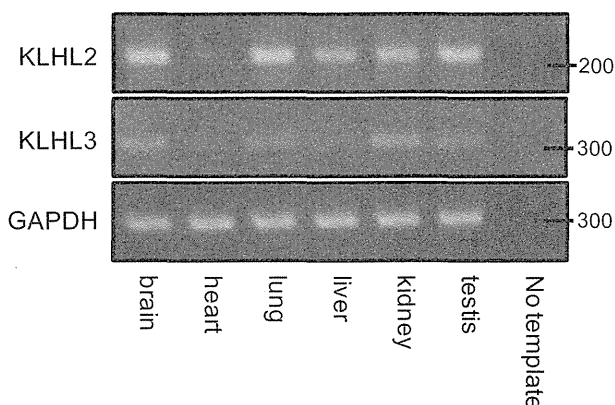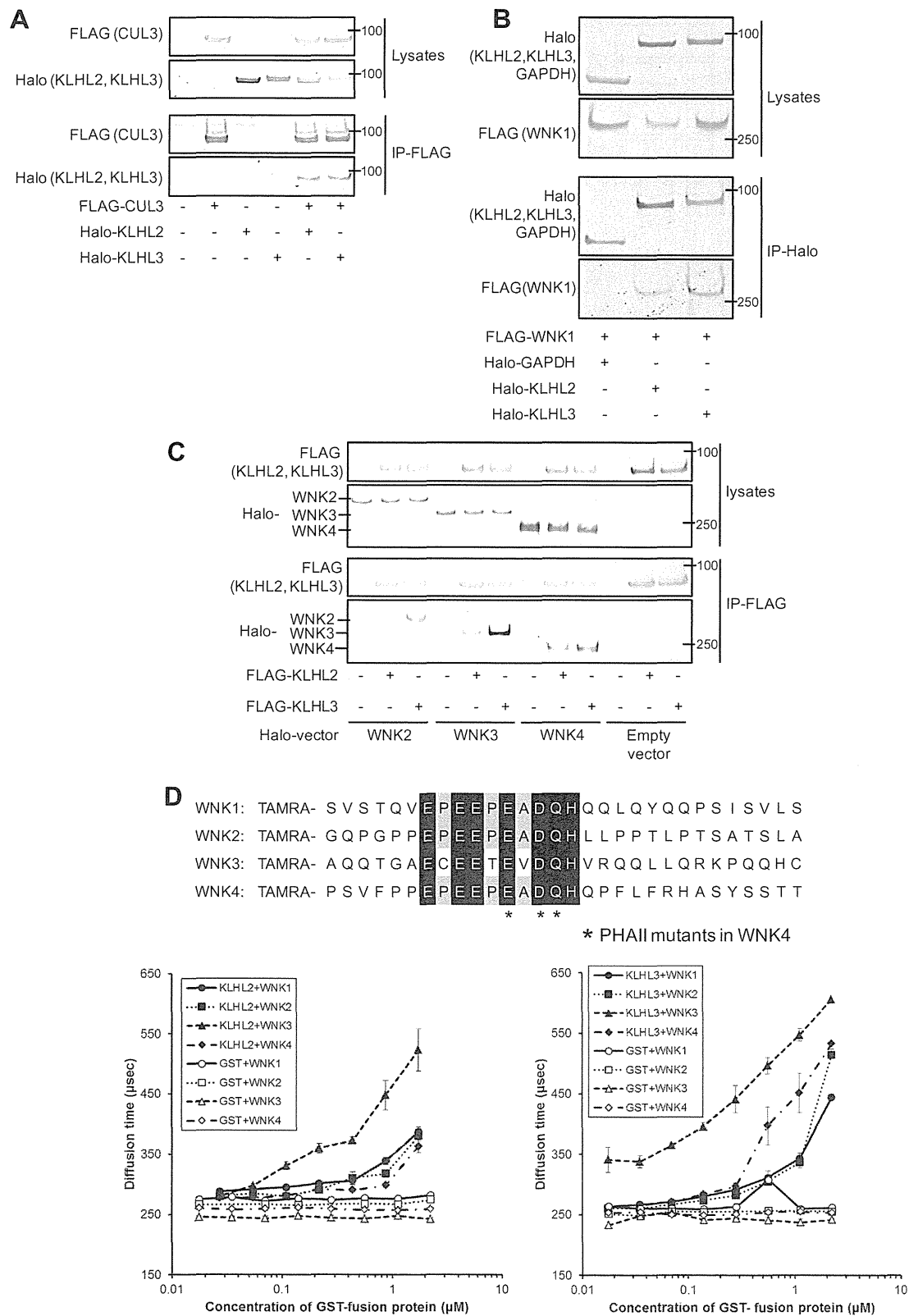
Fig. 2. KLHL2 interacted with Cullin3 and WNK kinases. (A) FLAG-tagged Cullin3 was co-immunoprecipitated with Halo-tagged KLHL2 as well as KLHL3 in HEK293T cells. (B) Halo-tagged KLHL2 and KLHL3 were co-immunoprecipitated with FLAG-tagged WNK1. (C) FLAG-tagged KLHL2 and KLHL3 were co-immunoprecipitated with Halo-tagged WNK2, WNK3 and WNK4. (D) Diffusion time of a single-molecule TAMRA-labeled peptide corresponding to the acidic domain of wild-type WNK kinases was measured by fluorescence correlation spectroscopy. The diffusion time of each peptide was significantly ($p < 0.05$) increased with KLHL2-GST at 0.21 μM or higher and KLHL3-GST at 0.14 μM or higher, but not with GST alone. These data indicate the direct binding of the Kelch-repeat of KLHL2 and KLHL3 to the acidic domain of WNK kinases.
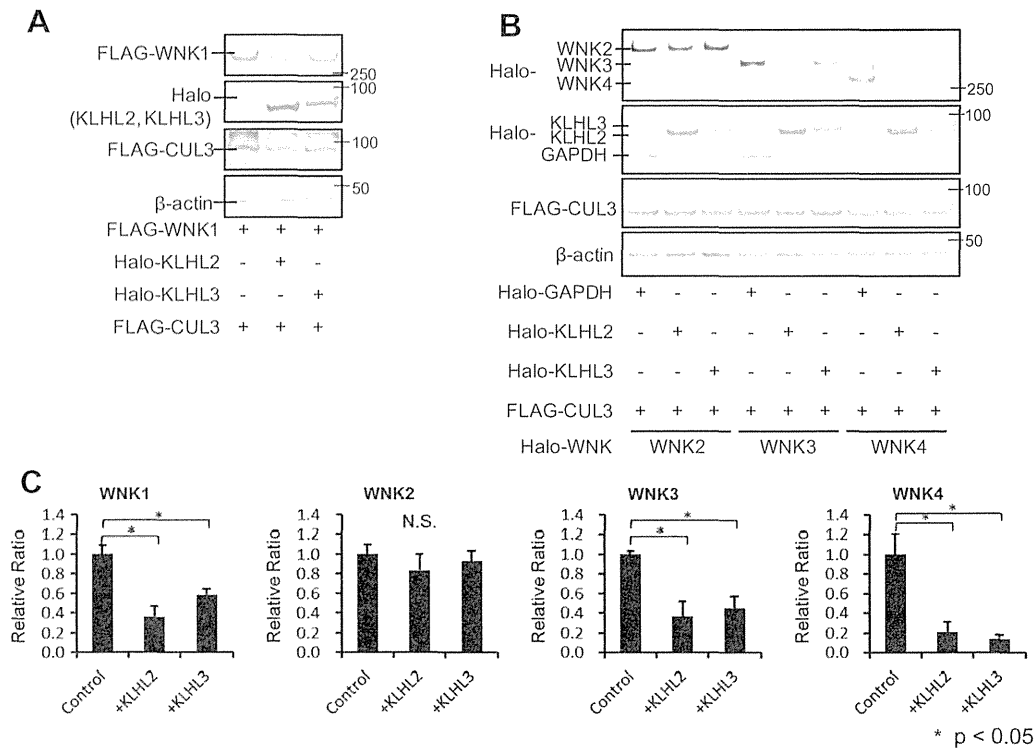
Fig. 3. KLHL2 regulated WNK kinase abundance. (A) FLAG-tagged WNK1 and FLAG-tagged Cullin3 were co-expressed with Halo-tagged KLHL2 or KLHL3. Co-expression of KLHL2 as well as KLHL3 decreased the abundance of WNK1. (B) Halo-tagged WNK kinases and FLAG-tagged Cullin3 were co-expressed with Halo-tagged GAPDH, KLHL2 or KLHL3. The cellular WNK3 and WNK4 abundance were decreased by co-expression of KLHL2 or KLHL3. The WNK2 was not affected by the co-expression. (C) Densitometric analysis of the results of (A) and (B). *$p < 0.05$ compared with control.
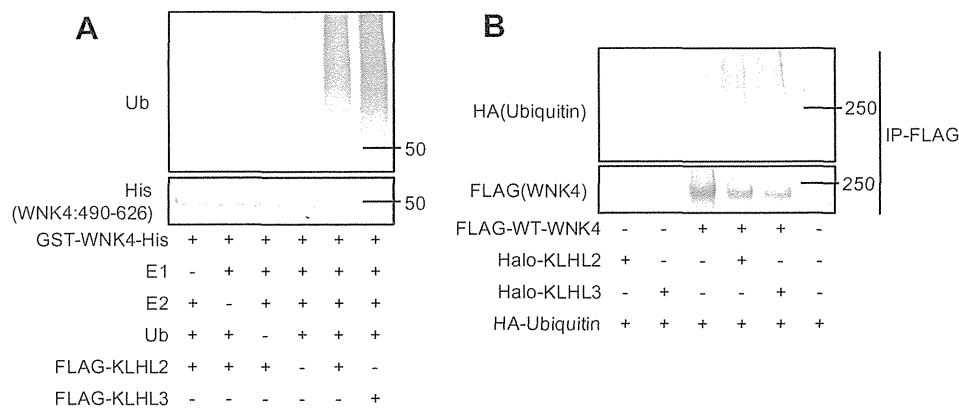
Fig. 4. KLHL2 increased WNK4 ubiquitination. (A) In vitro ubiquitination assay of WNK4. WNK4 (490–626) (50 kDa) was incubated with ubiquitin, E1 and E2 (UbcH5a/UBE2D1) with or without KLHL2–Cullin3 or KLHL3–Cullin3 complex. KLHL2 as well as KLHL3 significantly ubiquitinated WNK4 (490–626) in vitro. (B) WNK4 was expressed with HA-ubiquitin and KLHL2 or KLHL3, and immunoprecipitated under a denaturing condition. As shown in the ubiquitin (HA) immunoblot, the ubiquitination signals were observed as a smeared band over the apparent molecular size of WNK4 (200 kDa). The ubiquitination of WNK4 was increased by co-expression of KLHL2 or KLHL3.

of other WNKs by KLHL2 and/or KLHL3 may be involved in certain pathophysiological conditions in extrarenal tissues.

In summary, we have identified the function of KLHL2 as an E3 ubiquitin ligase for WNK kinases. Different combinations of KLHL2 and KLHL3 with WNKs could regulate WNK kinase signaling in different kinds of cells.

Appendix A. Supplementary data

Supplementary data associated with this article can be found, in the online version, at http://dx.doi.org/10.1016/j.bbrc.2013.06.104.

References

[1] F.H. Wilson, S. Disse-Nicodème, K.A. Choate, K. Ishikawa, C. Nelson-Williams, I. Desitter, M. Gunel, D.V. Milford, G.W. Lipkin, J.M. Achard, M.P. Feely, B. Dussol, Y. Berland, R.J. Unwin, H. Mayan, D.B. Simon, Z. Farfel, X. Jeunemaitre, R.P. Lifton, Human hypertension caused by mutations in WNK kinases, Science 293 (2001) 1107–1112.

[2] R.D. Gordon, The syndrome of hypertension and hyperkalemia with normal glomerular filtration rate: Gordon's syndrome, Aust. N.Z. J. Med. 16 (1986) 183–184.

[3] C. Richardson, D.R. Alessi, The regulation of salt transport and blood pressure by the WNK-SPAK/OSR1 signalling pathway, J. Cell Sci. 121 (2008) 3293–3304.

[4] S.S. Yang, T. Morimoto, T. Rai, M. Chiga, E. Sohara, M. Ohno, K. Uchida, S.H. Lin, T. Moriguchi, H. Shibuya, Y. Kondo, S. Sasaki, S. Uchida, Molecular pathogenesis of pseudohypoaldosteronism type II: generation and analysis of a Wnk4(D561A/+) knockin mouse model, Cell Metab. 5 (2007) 331–344.

[5] M. Chiga, T. Rai, S.S. Yang, A. Ohta, T. Takizawa, S. Sasaki, S. Uchida, Dietary salt regulates the phosphorylation of OSR1/SPAK kinases and the sodium chloride cotransporter through aldosterone, Kidney Int. 74 (2008) 1403–1409.

[6] A. Ohta, T. Rai, N. Yui, M. Chiga, S.S. Yang, S.H. Lin, E. Sohara, S. Sasaki, S. Uchida, Targeted disruption of the Wnk4 gene decreases phosphorylation of Na-Cl cotransporter, increases Na excretion and lowers blood pressure, Hum. Mol. Genet. 18 (2009) 3978–3986.

[7] M. Castañeda-Bueno, L.G. Cervantes-Pérez, N. Vázquez, N. Uribe, S. Kantesaria, L. Morla, N.A. Bobadilla, A. Doucet, D.R. Alessi, G. Gamba, Activation of the renal Na+:Cl− cotransporter by angiotensin II is a WNK4-dependent process, Proc. Natl. Acad. Sci. USA 109 (2012) 7929–7934.

[8] L.M. Boyden, M. Choi, K.A. Choate, C.J. Nelson-Williams, A. Farhi, H.R. Toka, I.R. Tikhonova, R. Bjornson, S.M. Mane, G. Colussi, M. Lebel, R.D. Gordon, B.A. Semmekrot, A. Poujol, M.J. Välimäki, M.E. De Ferrari, S.A. Sanjad, M. Gutkin, F.E. Karet, J.R. Tucci, J.R. Stockigt, K.M. Keppler-Noreuil, C.C. Porter, S.K. Anand, M.L. Whiteford, I.D. Davis, S.B. Dewar, A. Bettinelli, J.J. Fadrowski, C.W. Belsha, T.E. Hunley, R.D. Nelson, H. Trachtman, T.R. Cole, M. Pinsk, D. Bockenhauer, M. Shenoy, P. Vaidyanathan, J.W. Foreman, M. Rasoulpour, F. Thameem, H.Z. Al-Shahrouri, J. Radhakrishnan, A.G. Gharavi, B. Goilav, R.P. Lifton, Mutations in kelch-like 3 and Cullin 3 cause hypertension and electrolyte abnormalities, Nature 482 (2012) 98–102.

[9] H. Louis-Dit-Picard, J. Barc, D. Trujillano, S. Miserey-Lenkei, N. Bouatia-Naji, O. Pylypenko, G. Beaurain, A. Bonnefond, O. Sand, C. Simian, E. Vidal-Petiot, C. Soukaseum, C. Mandet, F. Broux, O. Chabre, M. Delahousse, V. Esnault, B. Fiquet, P. Houillier, C.I. Bagnis, J. Koenig, M. Konrad, P. Landais, C. Mourani, P. Niaudet, V. Probst, C. Thauvin, R.J. Unwin, S.D. Soroka, G. Ehret, S. Ossowski, M. Caulfield, P. Bruneval, X. Estivill, P. Froguel, J. Hadchouel, J.J. Schott, X. Jeunemaitre, I.C.f.B.P. (ICBP), KLHL3 mutations cause familial hyperkalemic hypertension by impairing ion transport in the distal nephron, Nat. Genet. 44 (2012) 456–460. S451–S453.

[10] M. Furukawa, Y. Xiong, BTB protein Keap1 targets antioxidant transcription factor Nrf2 for ubiquitination by the Cullin 3-Roc1 ligase, Mol. Cell. Biol. 25 (2005) 162–171.

[11] Y.R. Lee, W.C. Yuan, H.C. Ho, C.H. Chen, H.M. Shih, R.H. Chen, The Cullin 3 substrate adaptor KLHL20 mediates DAPK ubiquitination to control interferon responses, EMBO J. 29 (2010) 1748–1761.

[12] M.Y. Lin, Y.M. Lin, T.C. Kao, H.H. Chuang, R.H. Chen, PDZ-RhoGEF ubiquitination by Cullin3–KLHL20 controls neurotrophin-induced neurite outgrowth, J. Cell Biol. 193 (2011) 985–994.

[13] M. Wakabayashi, T. Mori, K. Isobe, E. Sohara, K. Susa, Y. Araki, M. Chiga, E. Kikuchi, N. Nomura, Y. Mori, H. Matsuo, T. Murata, S. Nomura, T. Asano, H. Kawaguchi, S. Nonoyama, T. Rai, S. Sasaki, S. Uchida, Impaired KLHL3-mediated ubiquitination of WNK4 causes human hypertension, Cell Rep. 3 (2013) 858–868.

[14] S. Shibata, J. Zhang, J. Puthumana, K.L. Stone, R.P. Lifton, Kelch-like 3 and Cullin 3 regulate electrolyte homeostasis via ubiquitination and degradation of WNK4, Proc. Natl. Acad. Sci. USA (2013) 7838–7843.

[15] G. Wu, J.B. Peng, Disease-causing mutations in KLHL3 impair its effect on WNK4 degradation, FEBS Lett. (2013) 1717–1722.

[16] A. Ohta, F.R. Schumacher, Y. Mehellou, C. Johnson, A. Knebel, T.J. Macartney, N.T. Wood, D.R. Alessi, T. Kurz, The CUL3–KLHL3 E3 ligase complex mutated in Gordon's hypertension syndrome interacts with and ubiquitylates WNK isoforms: disease-causing mutations in KLHL3 and WNK4 disrupt interaction, Biochem. J. 451 (2013) 111–122.

[17] M. Soltysik-Espanola, R.A. Rogers, S. Jiang, T.A. Kim, R. Gaedigk, R.A. White, H. Avraham, S. Avraham, Characterization of Mayven, a novel actin-binding protein predominantly expressed in brain, Mol. Biol. Cell 10 (1999) 2361–2375.

[18] L.A. Tseng, J.L. Bixby, Interaction of an intracellular pentraxin with a BTB-Kelch protein is associated with ubiquitylation, aggregation and neuronal apoptosis, Mol. Cell. Neurosci. 47 (2011) 254–264.

[19] K. Yamauchi, T. Rai, K. Kobayashi, E. Sohara, T. Suzuki, T. Itoh, S. Suda, A. Hayama, S. Sasaki, S. Uchida, Disease-causing mutant WNK4 increases paracellular chloride permeability and phosphorylates claudins, Proc. Natl. Acad. Sci. USA 101 (2004) 4690–4694.

[20] A. Ohta, S.S. Yang, T. Rai, M. Chiga, S. Sasaki, S. Uchida, Overexpression of human WNK1 increases paracellular chloride permeability and phosphorylation of claudin-4 in MDCKII cells, Biochem. Biophys. Res. Commun. 349 (2006) 804–808.

[21] K. Kuroki, S. Kobayashi, M. Shiroishi, M. Kajikawa, N. Okamoto, D. Kohda, K. Maenaka, Detection of weak ligand interactions of leukocyte Ig-like receptor B1 by fluorescence correlation spectroscopy, J. Immunol. Methods 320 (2007) 172–176.

[22] P. Montague, P.G. Kennedy, S.C. Barnett, Subcellular localization of Mayven following expression of wild type and mutant EGFP tagged cDNAs, BMC Neurosci. 11 (2010) 63.

[23] S. Jiang, H.K. Avraham, S.Y. Park, T.A. Kim, X. Bu, S. Seng, S. Avraham, Process elongation of oligodendrocytes is promoted by the Kelch-related actin-binding protein Mayven, J. Neurochem. 92 (2005) 1191–1203.

[24] X. Bu, H.K. Avraham, X. Li, B. Lim, S. Jiang, Y. Fu, R.G. Pestell, S. Avraham, Mayven induces c-Jun expression and cyclin D1 activation in breast cancer cells, Oncogene 24 (2005) 2398–2409.

[25] S. Angers, C.J. Thorpe, T.L. Biechele, S.J. Goldenberg, N. Zheng, M.J. MacCoss, R.T. Moon, The KLHL12–Cullin-3 ubiquitin ligase negatively regulates the Wnt-beta-catenin pathway by targeting Dishevelled for degradation, Nat. Cell Biol. 8 (2006) 348–357.

[26] S. Prag, J.C. Adams, Molecular phylogeny of the kelch-repeat superfamily reveals an expansion of BTB/kelch proteins in animals, BMC Bioinformatics 4 (2003) 42.

[27] S.C. Lo, X. Li, M.T. Henzl, L.J. Beamer, M. Hannink, Structure of the Keap1:Nrf2 interface provides mechanistic insight into Nrf2 signaling, EMBO J. 25 (2006) 3605–3617.

Impaired KLHL3-Mediated Ubiquitination of WNK4 Causes Human Hypertension

Mai Wakabayashi,[1,4] Takayasu Mori,[1,4] Kiyoshi Isobe,[1] Eisei Sohara,[1] Koichiro Susa,[1] Yuya Araki,[1] Motoko Chiga,[1] Eriko Kikuchi,[1] Naohiro Nomura,[1] Yutaro Mori,[1] Hiroshi Matsuo,[2] Tomohiro Murata,[2] Shinsuke Nomura,[2] Takako Asano,[3] Hiroyuki Kawaguchi,[3] Shigeaki Nonoyama,[3] Tatemitsu Rai,[1] Sei Sasaki,[1] and Shinichi Uchida[1,*]

[1]Department of Nephrology, Graduate Schools of Medical and Dental Sciences, Tokyo Medical and Dental University, 1-5-45 Yushima, Bunkyo, Tokyo 113-8519, Japan
[2]Department of Cardiology and Nephrology, Mie University Graduate School of Medicine, 2-174 Edobashi, Tsu, Mie 514-8507, Japan
[3]Department of Pediatrics, National Defense Medical College, 3-2 Namiki, Tokorozawa, Saitama 359-8513, Japan
[4]These authors contributed equally to this work
*Correspondence: suchida.kid@tmd.ac.jp
http://dx.doi.org/10.1016/j.celrep.2013.02.024

SUMMARY

Mutations in WNK kinases cause the human hypertensive disease pseudohypoaldosteronism type II (PHAII), but the regulatory mechanisms of the WNK kinases are not well understood. Mutations in kelch-like 3 (*KLHL3*) and *Cullin3* were also recently identified as causing PHAII. Therefore, new insights into the mechanisms of human hypertension can be gained by determining how these components interact and how they are involved in the pathogenesis of PHAII. Here, we found that KLHL3 interacted with Cullin3 and WNK4, induced WNK4 ubiquitination, and reduced the WNK4 protein level. The reduced interaction of KLHL3 and WNK4 by PHAII-causing mutations in either protein reduced the ubiquitination of WNK4, resulting in an increased level of WNK4 protein. Transgenic mice overexpressing WNK4 showed PHAII phenotypes, and WNK4 protein was indeed increased in $Wnk4^{D561A/+}$ PHAII model mice. Thus, WNK4 is a target for KLHL3-mediated ubiquitination, and the impaired ubiquitination of WNK4 is a common mechanism of human hereditary hypertension.

INTRODUCTION

Hypertension is one of the biggest health problems in the industrialized world because it damages critical organs. Studies of monogenic hypertensive diseases, such as Liddle syndrome (Shimkets et al., 1994) and pseudohypoaldosteronism type II (PHAII) (Achard et al., 2001), have provided new insight into the mechanisms of blood pressure regulation in humans. Liddle syndrome is caused by mutations in the epithelial sodium channel (ENaC) that increase the amount of ENaC in the apical membranes of collecting ducts in the kidney through the impairment of ENaC ubiquitination, thereby increasing sodium reabsorption (Rossier and Schild, 2008). PHAII is another autosomal-dominant hereditary hypertensive disease that is characterized by hyperkalemia and metabolic acidosis (Gordon, 1986),

and genes encoding the WNK kinases (WNK1 and WNK4) were identified in 2001 as responsible (Wilson et al., 2001). However, the pathogenesis of PHAII was totally unknown when the WNK genes were identified. Since then, numerous in vitro and in vivo studies have been performed for clarifying the molecular pathogenesis of PHAII (Bergaya et al., 2011; Lalioti et al., 2006; Liu et al., 2011; McCormick and Ellison, 2011; Yang et al., 2003). We generated a mouse model of PHAII carrying the same mutation as patients with PHAII ($Wnk4^{D561A/+}$ knockin mouse) (Yang et al., 2007) and discovered that the constitutive activation of a novel signal cascade, consisting of WNK kinases, OSR1 and SPAK kinases, and the Na-Cl cotransporter (NCC), is the major pathogenic mechanism of PHAII (Chiga et al., 2008, 2011). However, the molecular pathogenesis of how the missense mutation of WNK4 activates the cascade remains to be clarified.

Recently, two new genes (*KLHL3* and *Cullin3*) were also identified as being associated with PHAII (Boyden et al., 2012; Louis-Dit-Picard et al., 2012). However, how these genes are involved in PHAII is unknown. Determining how these responsible genes (*WNK*, *KLHL3*, and *Cullin3*) are orchestrated and how pathogenic mutations in these genes cause a common hypertensive disease will contribute to the understanding of the molecular pathogenesis of human hypertension and also to the identification of new targets for antihypertensive drugs.

The purpose of the present study was to determine the pathogenic role of PHAII-causing mutations in the *WNK4*, *KLHL3*, and *Cullin3* genes. We found that WNK4 kinase is a substrate of KLHL3-Cullin3-targeted ubiquitination and that the PHAII-causing mutations of *WNK4* and *KLHL3* resulted in impaired WNK4 ubiquitination. The resultant increase in the WNK4 level was confirmed in $Wnk4^{D561A/+}$ PHAII model mice; this increase constitutively activates the WNK-OSR1/SPAK-NCC signal cascade and causes PHAII. Data from *WNK4* transgenic mice were consistent with this idea.

RESULTS

KLHL3 Interacted with and Regulated the Abundance of WNK4 Kinase Protein

We have reported that the activation of the WNK-OSR1/SPAK-NCC signal cascade is the major pathogenic mechanism of PHAII caused by a *WNK4* mutation (Yang et al., 2007), and
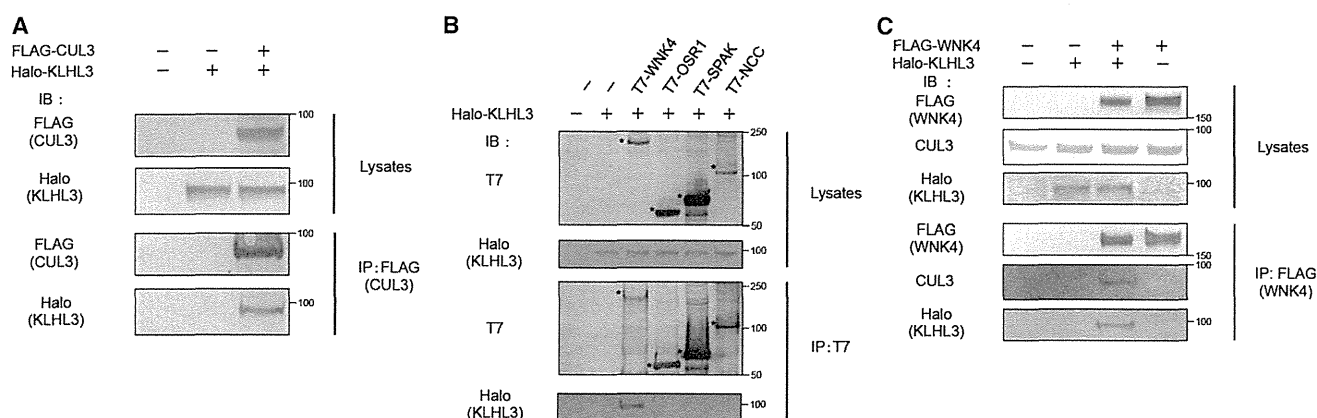
CrossMark

—146—

Figure 1. KLHL3 Was Coimmunoprecipitated with Cullin3 and WNK4
(A) FLAG-tagged Cullin3 (CUL3) was coimmunoprecipitated with Halo-tagged KLHL3 in HEK293T cells. IB, immunoblot; IP, immunoprecipitation.
(B) T7-tagged WNK4, OSR1, SPAK, and NCC were coexpressed with Halo-tagged KLHL3 in HEK293T cells and immunoprecipitated with T7 antibody. KLHL3 was coimmunoprecipitated only with WNK4. The asterisks indicate T7-tagged proteins.
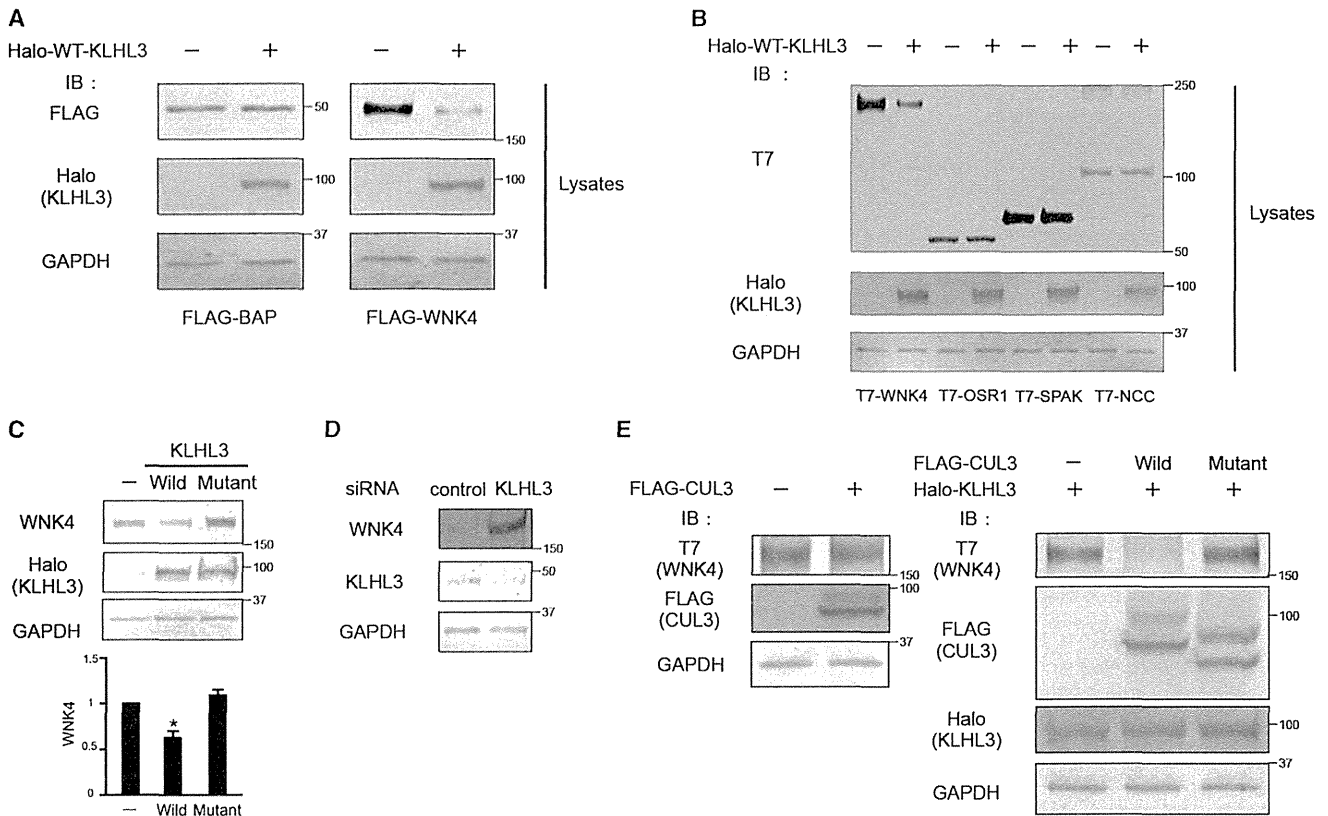(C) WNK4 was coimmunoprecipitated with endogenous Cullin3 in HEK293T cells in the presence of KLHL3 coexpression. Results similar to those shown in (A), (B), and (C) were obtained in three separate experiments.

mutations in the *KLHL3* and *Cullin3* genes were also reported as causing the same PHAII phenotypes (Boyden et al., 2012; Louis-Dit-Picard et al., 2012). These data suggest that KLHL3 and Cullin3 may somehow interact with the components of the WNK-OSR1/SPAK-NCC signal cascade. Because KLHL proteins function as substrate adaptors in Cullin3-based E3 ligase (Cirak et al., 2010; Kigoshi et al., 2011; Lee et al., 2010; Lin et al., 2011), we first confirmed a complex formation of KLHL3 and Cullin3 via coimmunoprecipitation (Figure 1A). We then investigated whether KLHL3 interacted with the components of the WNK-OSR1/SPAK-NCC signal cascade. To verify this, we performed coimmunoprecipitation assays of KLHL3 with WNK4, OSR1, SPAK, and NCC. As shown in Figure 1B, KLHL3 was coimmunoprecipitated with WNK4, but not with OSR1, SPAK, or NCC. The interaction of Cullin3 with WNK4 was also confirmed through coimmunoprecipitation when KLHL3 was overexpressed (Figure 1C), consistent with the previously reported role of KLHL proteins as substrate adaptors in the Cullin3-based ubiquitin E3 ligase (Cirak et al., 2010; Kigoshi et al., 2011; Lee et al., 2010; Lin et al., 2011). We tried to demonstrate coimmunoprecipitation of endogenous WNK4 and KLHL3 in kidney tissue and in cultured cells. However, this was not successful due to the relatively low level of expression of WNK4 in cultured cells and the lack of KLHL3 antibodies adequate for immunoprecipitation. The finding that WNK4 might be readily degraded by the binding to KLHL3 within cells as shown below also made the detection of coimmunoprecipitation difficult, especially in kidney samples.

To clarify the functional role of KLHL3 on WNK4, we overexpressed KLHL3 along with WNK4. As shown in Figure 2A, KLHL3 overexpression dramatically decreased WNK4 protein expression, even when overexpressed by a strong cytomegalovirus (CMV) promoter. The expression level of bacterial alkaline phosphatase (BAP) driven by the same promoter was not affected by KLHL3 coexpression. OSR1, SPAK, and NCC

expression levels were also not affected by KLHL3 coexpression (Figure 2B), supporting the results from the coimmunoprecipitation. To confirm the effect of KLHL3 on WNK4, we evaluated this effect on the endogenous WNK4 in mpkDCT cells, a mouse distal-tubule-derived cell line (Duong Van Huyen et al., 2001) (Figure 2C). Wild-type KLHL3 significantly decreased the endogenous WNK4 protein level. Conversely, KLHL3 knockdown significantly increased the WNK4 protein level (Figure 2D). Although these effects of KLHL3 expression on WNK4 were observed without Cullin3 overexpression, we further tested the effect of Cullin3 overexpression on WNK4 in human embryonic kidney 293T (HEK293T) cells. As shown in Figure 2E, coexpression of Cullin3 with KLHL3 further decreased the WNK4 protein level compared with the expression of KLHL3 alone. Cullin3 alone did not affect WNK4 abundance. These data suggested that the KLHL3-Cullin3 complex might be a strong regulator of the WNK4 protein abundance within cells. Although we tried to measure the half-life of WNK4 in the presence of KLHL3 and Cullin3, the robust decrease of WNK4 by KLHL3 and Cullin3 made the measurement extremely difficult. The difference could be highly significant based on the steady-state levels of transiently expressed WNK4, as shown in Figures 2A and 2B.

Next, we evaluated how a PHAII-causing mutation (R528H) of KLHL3 and Cullin3 affected the abundance of WNK4. When the expression levels of wild-type and mutant KLHL3 were similar, the R528H mutant was less able to reduce the endogenous protein level of WNK4 as compared to wild-type KLHL3 (Figure 2C). The PHAII-causing mutations of the *Cullin3* gene were reported to cause skipping of exon 9, which codes the segment (57 residues from 403–459) linking the BTB-binding and RING-binding domains of Cullin3 (Boyden et al., 2012). To investigate the pathogenic effect of the mutant Cullin3, we prepared Cullin3 lacking this segment. As shown in Figure 2E, the mutant Cullin3 was also less able to reduce WNK4 as compared to wild-type Cullin3.

A

Halo-WT-KLHL3   −   +   −   +

IB :

FLAG

Halo (KLHL3)

GAPDH

FLAG-BAP   FLAG-WNK4

Lysates

B

Halo-WT-KLHL3   − + − + − + − +

IB :

T7

Halo (KLHL3)

GAPDH

T7-WNK4 T7-OSR1 T7-SPAK T7-NCC

Lysates

C

KLHL3
− Wild Mutant

WNK4

Halo (KLHL3)

GAPDH

D

siRNA   control KLHL3

WNK4

KLHL3

GAPDH

E

FLAG-CUL3   −   +
IB :
T7 (WNK4)
FLAG (CUL3)
GAPDH

FLAG-CUL3   −   Wild   Mutant
Halo-KLHL3   +   +   +
IB :
T7 (WNK4)
FLAG (CUL3)
Halo (KLHL3)
GAPDH

Figure 2. Effect of Wild-Type and PHAII-Causing Mutant KLHL3 and Cullin3 Expression on Cellular WNK4 Abundance

(A) When coexpressed with KLHL3, the abundance of WNK4 protein within HEK293T cells expressed by CMV promoter (p3×FLAG-CMV-10 vector, Sigma-Aldrich) was dramatically decreased, whereas the abundance of BAP expressed by the same expression vector was not affected by KLHL3 coexpression.

(B) The reduction of WNK4 by KLHL3 coexpression was confirmed in another expression system of WNK4 (pRK5 vector), and OSR1, SPAK, and NCC levels were not affected by KLHL3 coexpression. Results similar to those shown in (A) and (B) were obtained in three separate experiments.

(C) Effect of wild-type and a PHAII-causing mutant (R528H) KLHL3 expression on the cellular abundance of WNK4. Endogenous WNK4 level in mpkDCT cells was decreased by wild-type KLHL3 expression. However, a similar level of the mutant KLHL3 expression failed to reduce WNK4 (*p < 0.05, compared with the WNK4 levels without KLHL3 coexpression [left lane] and with the mutant KLHL3 coexpression [right lane]; n = 3; mean ± SEM).

(D) Effect of the endogenous KLHL3 knockdown in mpkDCT cells on WNK4 expression. The protein levels of WNK4 were higher in KLHL3-knocked-down cells than in control cells. siRNA, small interfering RNA.

(E) Effect of wild-type and a PHAII-causing mutant *Cullin3* expression on the cellular abundance of WNK4. Although the expression of Cullin3 alone did not affect WNK4 protein level, Cullin3 expression with KLHL3 dramatically reduced WNK4 protein. The mutant *Cullin3* lacking the portion corresponding to exon 9 was less able to reduce WNK4 protein. The existence of two bands in the immunoblot of Cullin3 was reported previously (McEvoy et al., 2007). Similar results were obtained in three separate experiments.

PHAII-Causing Mutations of *WNK4* and *KLHL3* Affected the Interaction of WNK4 and KLHL3 and the Ubiquitination of WNK4

To investigate the mechanism(s) by which KLHL3 regulates the WNK4 protein level, we examined the ubiquitination of wild-type and PHAII-causing WNK4 with or without wild-type and mutant KLHL3. In this assay, we did not overexpress Cullin3, but used endogenous Cullin3 in HEK 293T cells (Figure 1C) because the overexpression of Cullin3 with KLHL3 robustly decreased WNK4 protein abundance (Figure 2E) under our experimental conditions, even in the presence of proteasome inhibitors, which made it difficult to recover WNK4 for immunoprecipitation. After coexpression of FLAG-tagged WNK4, Halo-tagged KLHL3, and hemagglutinin (HA)-tagged ubiquitin in HEK293T cells, the cells were treated with 1 μM epoxomicin,

and WNK4 was immunoprecipitated with FLAG antibody. First, we evaluated whether KLHL3 expression increased WNK4 ubiquitination. For the exclusion of ubiquitination signals from other proteins coimmunoprecipitated with WNK4, the immunoprecipitation was performed under a denaturing condition (Figure 3A). As previously shown in Figures 2A and 2B, when we expressed the wild-type KLHL3, the level of coexpressed wild-type WNK4 decreased significantly, even in the presence of a potent proteasome inhibitor (see WNK4 immunoblots of lysates and immunoprecipitated products in Figures 3A and 3C). As shown in the ubiquitin (HA) immunoblot (Figure 3A), the ubiquitination signals were observed as a smear band of over 200 kDa, which is the apparent molecular size of WNK4 (arrow). This data strongly suggested that WNK4 itself was indeed ubiquitinated, given that the immunoprecipitation was performed

under a denaturing condition. This ubiquitination was apparently increased by KLHL3 coexpression when the ubiquitination signals were corrected by the immunoprecipitated WNK4 abundance. To make the difference clear without correction, we adjusted the loading amount of the immunoprecipitated product to have the same amount of immunoprecipitated WNK4 in each lane in Figure 3A. A significant increase of WNK4 ubiquitination by KLHL3 was observed.

To further confirm that WNK4 was directly ubiquitinated by the KLHL3-Cullin3 complex, we performed an in vitro ubiquitination assay. Because the preparation of whole WNK4 protein was not successful, we prepared a portion of human WNK4 protein (residues from 490 to 626) containing the PHAII mutation sites as a GST fusion protein with a C-terminal His tag (50 kDa). As shown in the right panels of Figure 3A, we could confirm that the KLHL3-Cullin3 complex was able to directly ubiquitinate WNK4 (490–626).

Second, we tested the effect of the R528H KLHL3 mutation on WNK4 binding and ubiquitination. As already shown in Figure 2C, coexpression of wild-type KLHL3 significantly reduced WNK4 expression as compared with the mutant KLHL3 (Figure 3B, upper three panels). We observed a significant decrease in WNK4 ubiquitination by the mutant KLHL3 and also the decreased interaction of WNK4 with the mutant KLHL3 (Figure 3B, lower three panels).

We also tested the effect of PHAII-causing mutations of *WNK4* on WNK4-KLHL3 interaction and WNK4 ubiquitination. As shown in Figure 3A, wild-type KLHL3 decreased WNK4. However, this decrease mediated by KLHL3 was blunted in all three PHAII-causing *WNK4* mutants (Figure 3C, upper WNK4 panels). In the lower panels of Figure 3C, we showed the immnoblots of coimunoprecitated KLHL3 and ubiquitinated WNK4 after the loading adjustment as shown in Figures 3A and 3B. At the same time, we measured the signals before the loading adjustment and corrected the levels of WNK4 abundance as shown in Figure 3D. In either analysis, we could observe that the WNK4 mutants appeared to show less interaction with wild-type KLHL3 and less ubiquitination compared with wild-type WNK4. An in vitro ubiquitination assay using the wild-type and the mutant (D564A) WNK4 also supported this data (Figure S1).

The above data suggested that the acidic domain of WNK kinases (Figure 4), where PHAII mutants were clustered in WNK4, might be involved in the interaction with KLHL3. To investigate this hypothesis and to clarify whether the interaction of WNK4 and KLHL3 was direct, we measured the binding of TAMRA-labeled WNK4 peptide covering the acidic motif to the whole KLHL3 protein as a GST fusion protein in vitro. We used fluorescence correlation spectroscopy (FCS) to measure the diffusion time of the fluorescent peptide (FluoroPoint-Light, Olympus, Tokyo) (Kuroki et al., 2007), in the presence of different concentrations of GST-KLHL3. As shown in Figure 4, the diffusion time of TAMRA-labeled peptide became slower as the concentration of GST-KLHL3 increased, indicating that the WNK4 peptide bound to GST- KLHL3. GST alone did not affect the diffusion time, and the introduction of a PHAII-causing mutation (D564A) abolished the decrease in diffusion time by GST-KLHL3, clearly indicating that KLHL3 directly binds to WNK4.

WNK4 Protein Level Increased in the PHAII Model Mouse (*Wnk4$^{D561A/+}$*) Kidney

To determine whether the mechanism clarified in the cell culture studies was in fact working in the in vivo kidney, we re-evaluated our PHAII model mice carrying the D561A WNK4 mutation, which is equivalent to the human D564A mutation.

By using a recently generated WNK4 antibody that recognizes the amino terminus of WNK4 (Ohno et al., 2011), we found that the WNK4 protein level was significantly increased in the *Wnk4$^{D561A/+}$* mouse kidney (Figure 5A), which we missed in our initial report (Yang et al., 2007). The specificity of this WNK4 antibody was rigorously verified (Ohno et al., 2011) and also recently confirmed by using *WNK4* knockout mice (Figure S2). Furthermore, the *Wnk4$^{D561A/D561A}$* homozygous mouse showed a more increased WNK4 protein level, suggesting that the mutation may have a substantial effect in the regulation of the WNK4 protein level in vivo. We confirmed that the WNK4 messenger RNA (mRNA) level was not increased in the *Wnk4$^{D561A/D561A}$* homozygous mouse kidney (Figure 5B), indicating that the increase in the WNK4 protein level was not caused by transcriptional activation.

Increased Expression of WNK4 in the Kidney Induced the Activation of the WNK-OSR1/SPAK-NCC Signal Cascade

To confirm whether the increased WNK4 protein level activates OSR1/SPAK-NCC signaling in the kidney, we generated bacterial artificial chromosome (BAC)-transgenic (TG) mice harboring multiple copies of the wild-type *WNK4* gene, as previously reported (Lalioti et al., 2006). As shown in Figure 6A, we presented the results of two representative transgenic lines; one had a low copy number of the transgene (two copies) and the other had a high copy number (thirty copies). WNK4 protein levels in the kidneys of low copy number (LC) and high copy number (HC) TG mice were increased 1.7 ± 0.1 (mean ± SEM)-fold in LC-TG mice and 9.1 ± 0.2-fold in HC-TG mice (n = 5), compared with those of wild-type mice. The phosphorylation of OSR1, SPAK, and NCC in the kidney (Figure 6A) clearly increased as the WNK4 protein levels increased in the TG mice. Immunofluorescence of phosphorylated NCC and WNK4 also clearly showed the overexpression of WNK4 and the increased phosphorylation of NCC in the distal convoluted tubules (Figure S3), confirming the activation of WNK-OSR1/SPAK-NCC signaling in the TG mice. Nighttime systolic, diastolic, and mean blood pressure and daytime diastolic blood pressure were significantly increased as the WNK4 protein levels increased in the TG mice (Figure 6B). The blood pressure in these TG mice was also comparable to that of *Wnk4$^{D561A/+}$* knockin mice measured by the same telemetry system (wild-type versus *Wnk4$^{D561A/+}$* knockin: 118.3 ± 0.77 versus 125.1 ± 0.90, mean ±SEM, n = 4, p < 0.05). The LC-TG and HC-TG mice also showed hyperkalemia and metabolic acidosis (Table 1) like *Wnk4$^{D561A/+}$* knockin mice, and these phenotypes were more severe in HC-TG than LC-TG mice. We also investigated the phosphorylation status of NCC in two additional lines of transgene: one with no increase in WNK4 protein with two copies of the transgene, suggesting that the copy number of the transgene did not assure overexpression of the gene product, and the other with a robust
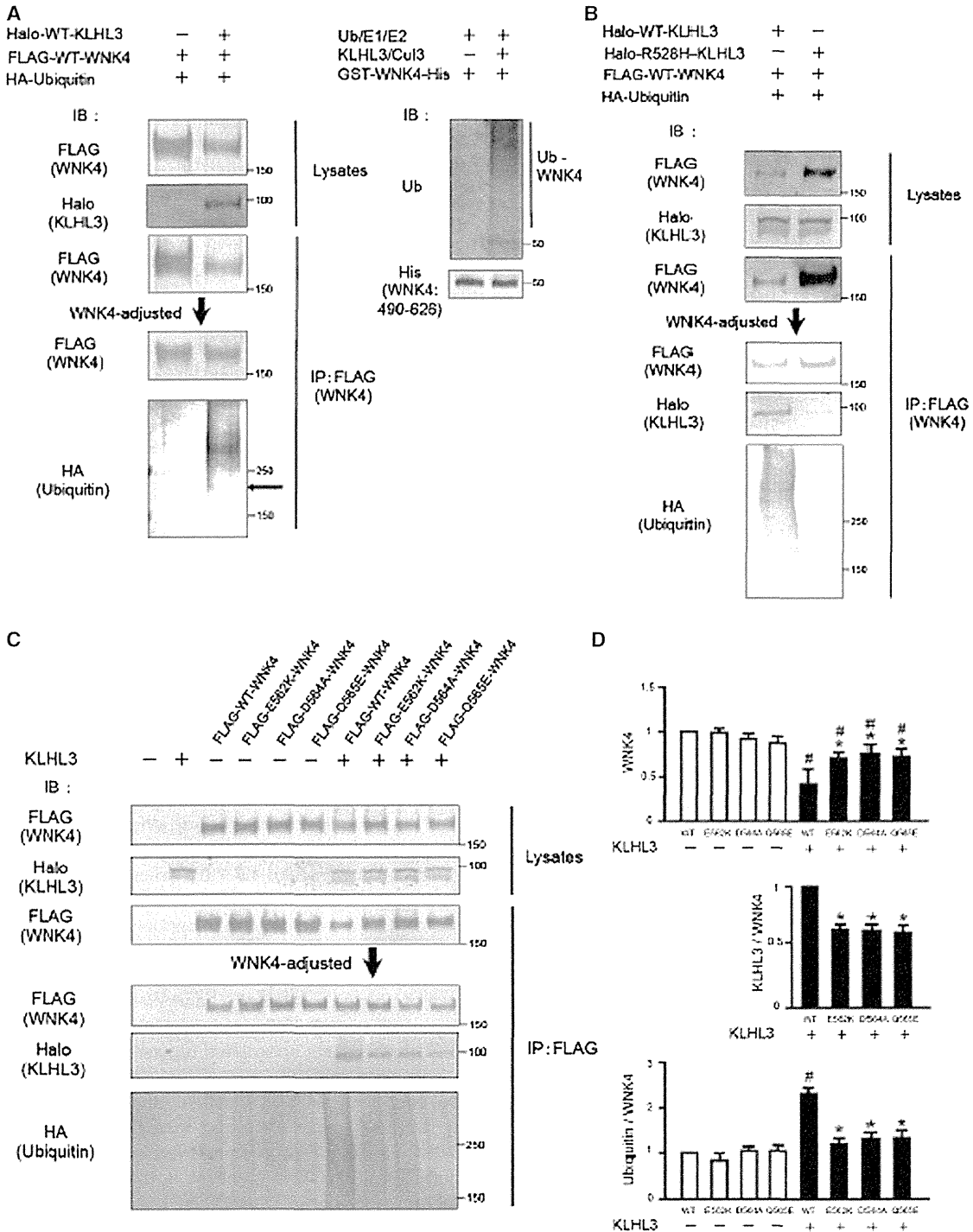
Figure 3. Effect of KLHL3 on the Ubiquitination of Wild-Type and PHAII-Causing Mutant WNK4

(A) Left panels: KLHL3 coexpression significantly induced the ubiquitination of wild-type WNK4. WNK4 was immunoprecipitated under a denaturing condition, and ubiquitinated WNK4 was observed as a smear band over 200 kDa, which is the apparent molecular size of WNK4 (arrow). Coexpression of wild-type KLHL3 significantly reduced the wild-type WNK4 level, even in the presence of 1 μM epoxomicin. Accordingly, in the lower panels, we reloaded the immunoprecipitated WNK4 samples to have equal amounts of immunoprecipitated WNK4 in each lane to demonstrate the difference in ubiquitination in each lane more clearly. We confirmed in the preliminary experiments that the data after loading adjustment faithfully reflected the data corrected by the immunoprecipitated WNK4 abundance before adjustment.

Right panels: In vitro ubiquitination assay of WNK4. WNK4 (490–626; 50 kDa) was incubated with ubiquitin, E1, and E2 (UbcH5a/UBE2D1) with or without the Cullin3-KLHL3 complex. Cullin3-KLHL3 significantly ubiquitinated WNK4 (490–626) in vitro. Similar results were obtained in three separate experiments.
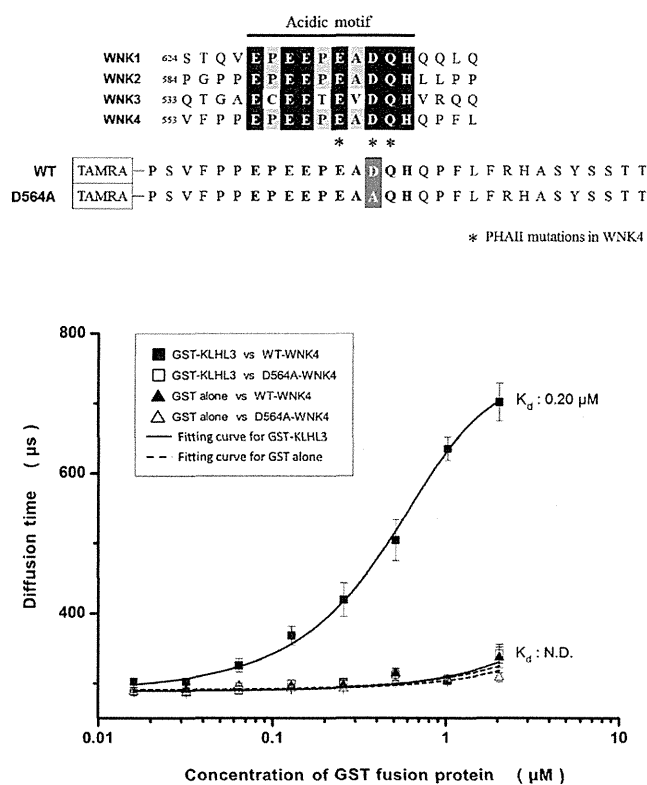
(legend continued on next page)

Acidic motif

WNK1 624 S T Q V E P E E P E A D Q H Q Q L Q
WNK2 584 P G P P E P E E P E A D Q H L L P P
WNK3 533 Q T G A E C E E T E V D Q H V R Q Q
WNK4 553 V F P P E P E E P E A D Q H Q P F L
                                    *   * *

WT | TAMRA |─ P S V F P P P E P E E P E A D Q H Q P F L F R H A S Y S S T T
D564A | TAMRA |─ P S V F P P P E P E E P E A A Q H Q P F L F R H A S Y S S T T

* PHAII mutations in WNK4

Figure 4. Direct Binding of KLHL3 to the Acidic Motif of Wild-Type WNK4

The diffusion time of a single-molecule TAMRA-labeled peptide corresponding to the acidic domain of wild-type WNK4 was measured by FCS. The addition of GST-KLHL3, not of GST only, dose-dependently increased the diffusion time, indicating the direct binding of KLHL3 to the acidic domain of WNK4 ($K_d = 0.20\ \mu M$). The diffusion time of a TAMRA-labeled peptide carrying a PHAII-causing mutation (D564A) was not affected by the addition of GST-KLHL3. The results are presented as means ± SEM (n = 5). N.D., not determined.

increase in WNK4 protein with twenty copies of the transgene. The increased phosphorylation of NCC was only observed in the line with WNK4 overexpression (Figure S4). These results clearly indicate that the activation of the WNK-OSR1/SPAK-NCC cascade and the induction of PHAII phenotypes were dependent on the increased WNK4 protein levels in the in vivo kidney.

A

B

Figure 5. Increased WNK4 Protein Levels in $Wnk4^{D561A/+}$ and $Wnk4^{D561A/D561A}$ Knockin Mice

(A) WNK4 in $Wnk4^{D561A/+}$ and $Wnk4^{D561A/D561A}$ mice was increased 2.2 ± 0.1- and 2.7 ± 0.2-fold, respectively, compared with that in wild-type mice (n = 6, mean ± SEM).

(B) *WNK4* transcription was not increased in the $Wnk4^{D561A/D561A}$ PHAII model mouse. Quantitative RT-PCR revealed that WNK4 mRNA levels in $Wnk4^{+/+}$ (open bar) and $Wnk4^{D561A/D561A}$ (closed bar) mouse kidneys were not statistically different (mean ± SEM; n = 6; p = 0.34). n.s., not significant. See also Figure S2.

DISCUSSION

We previously demonstrated the activation of the WNK-OSR1/SPAK-NCC phosphorylation cascade in the mouse model of PHAII, $Wnk4^{D561A/+}$ knockin mice (Yang et al., 2007), by developing phosphospecific antibodies for residues of the amino-terminal domain of NCC (Chiga et al., 2008; Yang et al., 2007). Then, we and others clarified that this signal cascade was important in blood pressure regulation under certain pathophysiological conditions other than PHAII (Hoorn et al., 2011; Komers et al., 2012; San-Cristobal et al., 2009; Sohara et al., 2011). Thus, there is wide agreement (Gamba, 2012) that the phosphorylation status of NCC governed by WNK-OSR1/SPAK signaling reflects NCC activity in vivo. Given that PHAII is a thiazide-sensitive disease, we speculated that *KLHL3* and *Cullin3* mutations

---

(B) Effect of wild-type and a PHAII-causing mutant KLHL3 expression on WNK4-KLHL3 binding and WNK4 ubiquitination. Upper panels: as shown in Figure 2C, wild-type KLHL3 reduced the coexpressed WNK4 protein level more significantly than did the mutant KLHL3, even in the presence of 1 μM epoxomicin. Accordingly, as in Figure 3A, the immunoprecipitated WNK4 samples were reloaded for equal amounts of immunoprecipitated WNK4 in each lane (lower panels). The binding of WNK4 to mutant KLHL3 and WNK4 ubiquitination by the mutant KLHL3 were significantly impaired. The immunoprecipitation was performed under a nondenaturing condition for assessing the binding to KLHL3 in the same experiments. Similar results were obtained in three separate experiments.

(C) Effect of PHAII-causing mutations of *WNK4* on WNK4-KLHL3 binding and WNK4 ubiquitination. As shown in Figure 3A, coexpression of wild-type KLHL3 significantly reduced the wild-type WNK4 level, even in the presence of 1 μM epoxomicin. However, this decrease was blunted in PHAII-causing *WNK4* mutations (see WNK4 immunoblots of lysates or immunoprecipitates in the upper panels). All three PHAII-causing WNK4 mutants showed less ubiquitination and less binding to KLHL3 (see quantification of blots in D).

(D) Quantification of the results showing the comparison of WNK4 ubiquitination and WNK4 binding to KLHL3 among wild-type and PHAII-causing WNK4 mutants. Upper graph, immunoprecipitated WNK4 abundance; middle graph, coimmunoprecipitated KLHL3 corrected by WNK4 abundance; lower graph, WNK4 ubiquitination corrected by WNK4 abundance. WNK4 ubiquitination was evaluated by separate sets of immunoprecipitation experiments under a denaturing condition. Data before loading adjustment were used for quantification. (#p < 0.05 compared with wild-type [WT]-WNK4 without KLHL3; *p < 0.05 compared with WT-WNK4 with KLHL3; n = 3; mean ± SEM). See also Figure S1.

A

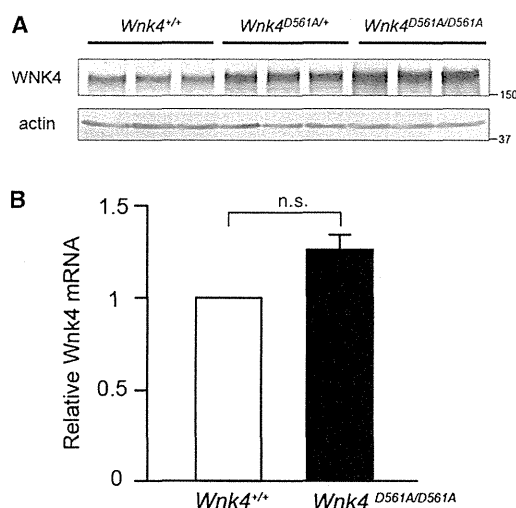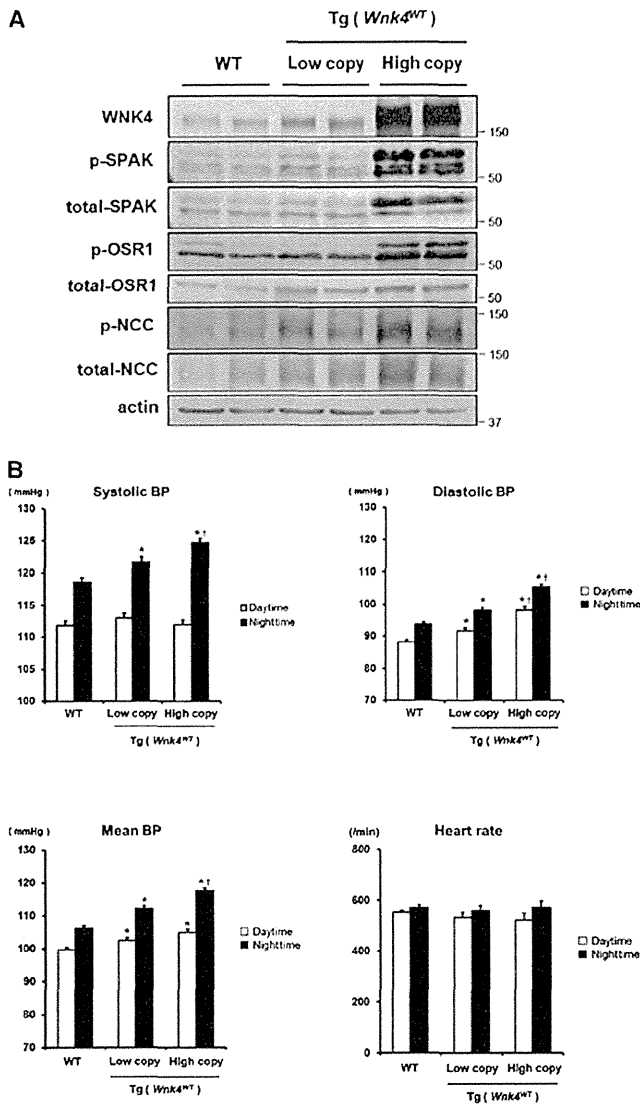**B**

Figure 6. Generation and Analysis of WNK4 TG Mice
(A) Status of the WNK-OSR1/SPAK-NCC phosphorylation cascade in the WNK4 TG mice (Tg(Wnk4^{WT})). WNK4 protein levels in the kidneys of LC (two copies) and HC (thirty copies) TG mice were increased 1.7 ± 0.1- and 9.1 ± 0.2-fold, respectively (*$p < 0.05$, $n = 5$, mean $\pm$ SEM). NCC phosphorylation in these mice was significantly increased, compared with that of wild-type mice ($p < 0.05$, $n = 5$, mean $\pm$ SEM). The phosphorylation of SPAK in LC-TG and HC-TG mice and that of OSR1 in HC-TG mice was also significantly increased compared to that of wild-type mice ($p < 0.05$, $n = 5$, mean $\pm$ SEM). The total and phosphorylated OSR1, SPAK, and NCC in HC-TG mice were significantly increased compared with those in LC-TG mice ($p < 0.05$, $n = 5$, mean $\pm$ SEM).
(B) Nighttime systolic, diastolic, and mean blood pressure (BP) and daytime diastolic blood pressure were significantly increased as the WNK4 protein levels increased in the Tg(Wnk4^{WT}) mice. Values were collected over 7 consecutive days (daytime: from 8:00 until 20:00; nighttime: from 20:00 until 8:00). *$p < 0.05$ versus WT; †$p < 0.05$ versus LC; WT $n = 5$; LC-TG $n = 5$; HC-TG $n = 4$; mean $\pm$ SEM.
See also Figures S3 and S4.

would also activate the WNK-OSR1/SPAK-NCC phosphorylation cascade. Gamba's group also recently clarified that the major WNK kinase regulating NCC phosphorylation in the kidney

Table 1. Blood Biochemistries of WT and LC- and HC-Tg(Wnk4^{WT}) Mice

	WT Mice (n = 16)	LC (n = 16) Tg(Wnk4^{WT}) Mice	HC (n = 16) Tg(Wnk4^{WT}) Mice
Na (mmol/l)	145.4 ± 0.3	147.0 ± 0.3*	147.4 ± 0.5**
K (mmol/l)	4.2 ± 0.1	5.1 ± 0.1**	5.5 ± 0.1**,†
Cl (mmol/l)	110.3 ± 0.3	111.9 ± 0.3**	112.8 ± 0.5**
HCO$_3^-$ (mmol/l)	24.4 ± 0.3	21.5 ± 0.4**	21.1 ± 0.3**
pH (venous)	7.302 ± 0.023	7.245 ± 0.003**	7.220 ± 0.004**,††

Values are the mean $\pm$ SEM. *, $p < 0.05$; **, $p < 0.01$ versus wild-type (WT) (one-way ANOVA followed by Tukey's post hoc test). †, $p < 0.05$; ††, $p < 0.01$ versus low copy number (one-way ANOVA followed by Tukey's test). Low copy number (LC) and high copy number (HC) Tg(Wnk4^{WT}) mice showed hyperkalemia and metabolic acidosis.

is WNK4 (Castañeda-Bueno et al., 2012). Accordingly, we first performed coimmunoprecipitation assays of KLHL3 with the components of the WNK4-OSR1/SPAK-NCC cascade because KLHL proteins have been recently identified as substrate adaptors in the Cullin3-based ubiquitin E3 ligase (Cirak et al., 2010; Kigoshi et al., 2011; Lee et al., 2010; Lin et al., 2011).

We found that KLHL3 showed a clear interaction only with WNK4 among the components of the cascade. The direct binding of WNK4 to KLHL3 at the acidic motif was also confirmed in this study. In addition to the interaction, we showed that KLHL3 coexpression dramatically reduced both overexpressed and endogenous WNK4, indicating that KLHL3 is a strong regulator of WNK4 protein abundance within cells. Such an effect was reduced in the PHAII-causing mutations of WNK4 and KLHL3, resulting in a common consequence: the increase in WNK4 protein abundance. We also confirmed that the interaction of KLHL3 with WNK4 induced the ubiquitination of WNK4 in HEK293T cells and in in vitro ubiquitination assay. The reduced interaction of KLHL3 with WNK4 by PHAII-causing mutations in either protein also reduced the ubiquitination of WNK4, and the PHAII-causing mutant Cullin3 was less able to reduce WNK4 protein abundance. Although we cannot exclude the possibility that KLHL3 may have targets other than WNK4, these results strongly suggest that WNK4 protein abundance within cells is regulated by KLHL3-Cullin3-mediated ubiquitination of WNK4 and that the major common molecular mechanism of PHAII is the impaired ubiquitination of WNK4.

Because the in vitro data could explain the molecular pathogenesis of PHAII caused by three different kinds of molecules, i.e., WNK4, KLHL3, and Cullin3, we verified this idea in vivo. Previously, WNK4 was shown to be able to phosphorylate and activate OSR1 and SPAK, as well as WNK1, in vitro (Moriguchi et al., 2005), and Ahlstrom and Yu (2009) reported in HEK293 cells that the intrinsic kinase activity of PHAII-causing mutant WNK4 was not different from that of wild-type WNK4. Given that the recent data on WNK4 knockout mice (Castañeda-Bueno et al., 2012) clearly indicate that WNK4 is the major WNK kinase in the kidney, we think it is reasonable to infer that the increased WNK4 abundance in the kidney, as we observed in the Wnk4$^{D561A/+}$ mice, could activate the cascade and was the cause of PHAII. To further prove this idea, we generated wild-

type WNK4-TG mice as previously reported (Lalioti et al., 2006). We evaluated several lines of TG mice with different levels of WNK4 protein overexpression, and we think that WNK4 TG mice could mimic $Wnk4^{D561A/+}$ knockin mice. We clearly showed that the WNK-OSR1/SPAK-NCC cascade and the PHAII phenotypes were induced according to the increases in wild-type WNK4 protein overexpression. This WNK4-dependent expression of phenotypes strongly suggests that these phenotypes were not caused by a nonspecific effect of the transgene. Several studies, mainly performed in Xenopus oocytes and in cultured cells, have shown that WNK4 behaves as a negative regulator of NCC (Wilson et al., 2003; Yang et al., 2003). This negative effect was shown to be a kinase-activity-independent function of WNK4 (Yang et al., 2005), suggesting that the kinase-activity-dependent positive and -activity-independent negative effects of WNK4 might act on NCC concomitantly and that the net effect might differ in different experimental situations. In fact, the WNK4-TG mouse with the wild-type WNK4 gene generated by Lalioti et al. (2006) was reported to show Gitelman-syndrome-like phenotypes rather than those of PHAII, which is contrary to our TG data in this study. No data regarding the status of the WNK-OSR1/SPAK-NCC cascade and WNK4 protein level in their TG mice have been reported (Lalioti et al., 2006). In addition, it was not clear whether the negative effect of wild-type WNK4 on NCC was dependent on WNK4 protein levels, because only a single line of TG mice was reported. Therefore, the reason for the discrepancy between our WNK4 TG study and Lalioti's study is not clear. It is possible that the level of WNK4 protein in their TG mice might be less than those in our WNK4 TG mice and PHAII models (about 2-fold increases); they mentioned that only a 50% increase in WNK4 mRNA expression was observed in their TG mice. The net effect of WNK4 on NCC might be expressed as a negative effect under such conditions. Our previous study using the triple knockin mice of WNK4, OSR1, and SPAK suggested that the contribution of this negative effect of WNK4 on NCC might be minimal in the kidney, at least under PHAII conditions (Chiga et al., 2011). Our TG data in this study also clearly indicate that the increase in WNK4 protein at the PHAII level or higher brought about a positive net effect on NCC.

Because NCC phosphorylation in the kidney is highly dependent on WNK4 (Castañeda-Bueno et al., 2012; Oi et al., 2012; Susa et al., 2012), we focused on WNK4 in this study. However, WNK kinases other than WNK4 may also be regulated by the KLHL3-Cullin3 complex. The amino acid sequence of the KLHL3 binding site in WNK4 is highly conserved in other WNK kinases (Figure 4), and we could observe that WNK1 protein, as well as WNK4 protein, was decreased by overexpression and increased by knockdown of KLHL3 (Figure S5). In this respect, WNK1 as well as WNK4 may be increased in the kidneys of patients with PHAII carrying the KLHL3 and Cullin3 mutations, thereby contributing to the activation of OSR1/SPAK-NCC signaling and to more severe PHAII phenotypes via Cullin3 and KLHL3 than those via WNK1 and WNK4 (Boyden et al., 2012). Because the PHAII-causing mutations of WNK1 are the large deletions of intron 1, which reportedly increases WNK1 transcription (Wilson et al., 2001), the mechanism clarified in this study may not be directly related to the pathogenesis of PHAII

by the WNK1 mutations. However, we may consider PHAII as a disease caused by increased WNK kinase abundance either by the dysregulation of transcription or by the ubiquitination of WNK kinases.

In summary, our study identified that WNK4 is a substrate of KLHL3-Cullin3-mediated ubiquitination and that the impaired ubiquitination of WNK4 is a common mechanism of PHAII by WNK4, KLHL3, and Cullin3 PHAII-causing mutations. Additional studies may be necessary to confirm this pathogenic mechanism in vivo by generating KLHL3 and Cullin3 knockin mice carrying PHAII mutations.

EXPERIMENTAL PROCEDURES

Plasmids

Expression plasmids for 3×FLAG-tagged human WNK4 and 3×FLAG-tagged D564A human WNK4 have been described previously (Yamauchi et al., 2004). E562K and Q565E mutations were also introduced by using a QuikChange Site-Directed Mutagenesis Kit (Stratagene). The complementary DNA (cDNA) encoding Halo-tagged human KLHL3 in pFN21A vector (HT-KLHL3) was purchased from Promega, and a disease-causing mutation (R528H) was introduced. Human Cullin3 cDNA was isolated by RT-PCR using human prostate mRNA as a template, and the cDNA was cloned into 3×FLAG-CMV10 vector (Sigma-Aldrich). T7-tagged OSR1, T7-tagged SPAK, and T7-tagged NCC expression plasmids in pRK5 vector were kindly provided by T. Moriguchi and H. Shibuya (Moriguchi et al., 2005). T7-tagged human WNK4 construct was also generated by introducing the T7 epitope by PCR. HA$_4$-tagged ubiquitin expression vector was kindly provided by T. Ohta (St. Marianna University School of Medicine).

Cell Culture and Transfections

HEK293T cells were cultured in Dulbecco's modified Eagle's medium supplemented with 10% (v/v) fetal bovine serum, 2 mM L-glutamine, 100 U/ml penicillin, and 0.1 mg/ml streptomycin at 37°C in a humidified 5% CO_2 incubator. The mpkDCT cell line kindly provided by A. Vandewalle was cultured in a defined medium as described previously (Duong Van Huyen et al., 2001). HEK293T cells and mpkDCT cells (3 × 10^5 cells per 6 cm dish) were transfected by the indicated amount of plasmid DNA with Lipofectamine 2000 reagent (Invitrogen). For each transfection, 4~8 μg of expression vectors were used, and the total amount of plasmid DNA was adjusted by adding empty vectors. In preliminary experiments, FLAG-tagged BAP (Figure 2A) was used for evaluating the transfection efficiency of transient expression of FLAG-tagged WNK4.

Immunoprecipitation

HEK293T cells transfected with the indicated amount of DNA were lysed in a buffer (50 mM Tris-HCl [pH 7.5], 150 mM NaCl, 1% Nonidet P-40, 1 mM sodium orthovanadate, 50 mM sodium fluoride, and protease inhibitor cocktail) for 30 min at 4°C. When the cells were transfected with the HA-ubiquitin expression plasmid, the cells were treated with 1 μM epoxomicin (specific and irreversible proteasome inhibitor; Peptide Institute, Osaka, Japan) for 3 hr before harvesting. After centrifugation at 12,000 × g for 15 min, the protein concentration of the supernatants was measured, and equal amounts of the supernatants were used for immunoprecipitation with anti-FLAG M2 beads (Sigma-Aldrich) or anti-T7 beads (Merck Millipore) for 2 hr at 4°C. Thereafter, the precipitants were washed with the lysis buffer and the immunoprecipitates were eluted in SDS sample buffer after boiling for 5 min. To detect ubiquitination of WNK4 in denatured samples, the cells transfected with various plasmids were lysed in 2% SDS buffer (2% SDS, 150 mM NaCl, 10 mM Tris-HCl [pH 8.0], 2 mM sodium orthovanadate, 50 mM sodium fluoride, and 1× protease inhibitors) and boiled for 10 min, followed by sonication. Before immunoprecipitation, the lysates were diluted 1:10 in a dilution buffer (10 mM Tris-HCl [pH 8.0], 150 mM NaCl, 2 mM EDTA, and 1% Triton X-100), incubated at 4°C for 1 hr with rotation, and centrifuged at 12,000 × g for 15 min.

Immunoblotting

Whole homogenates of mouse kidney without the nuclear fraction (600 × g) or the crude membrane fraction (17,000 × g) were subjected to semiquantitative immunoblotting, as described previously (Yang et al., 2007). Cells transfected with the indicated amount of plasmid DNA were lysed in lysis buffer (50 mM Tris-HCl [pH 7.5], 150 mM NaCl, 1% Nonidet P-40, 1 mM sodium orthovanadate, 50 mM sodium fluoride, and protease inhibitor cocktail [Roche Diagnostics]) for 30 min at 4°C. After centrifugation at 12,000 × g for 15 min, the supernatants were boiled with SDS sample buffer (Cosmo Bio USA) and subjected to SDS-PAGE. Blots were probed with the following primary antibodies: anti-total NCC (Ohno et al., 2011), anti-phosphorylated NCC (pSer71) (Yang et al., 2007), anti-WNK4 (Ohno et al., 2011; Ohta et al., 2009), anti-total OSR1 (M9; Abnova), anti-phosphorylated OSR1 (Ohta et al., 2009), anti-total SPAK (Cell Signaling Technology), anti-phosphorylated SPAK (Yang et al., 2010), anti-GAPDH (Santa Cruz Biotechnology), anti-actin (Cytoskeleton), anti-HA (Merck Millipore), anti-KLHL3 (Abcam), anti-Cullin3 (Abcam), anti-FLAG (Sigma-Aldrich), anti-Halo (Promega), and anti-T7 (Merck Millipore). Specificities of anti-pNCC, pOSR1, and pSPAK were rigorously determined in our previous reports (Chiga et al., 2008; Ohta et al., 2009; Yang et al., 2007, 2010). Alkaline-phosphatase-conjugated immunoglobulin G antibodies (Promega) were used as secondary antibodies for immunoblotting. The intensity of the bands was analyzed and quantified by using ImageJ software (National Institutes of Health).

In Vitro Ubiquitination Assay

cDNA encoding human WNK4 (490–626) with a C-terminal His-tag was amplified by PCR and cloned into pGEX6p-1 vector. Recombinant GST fusion WNK4 protein was expressed in BL21 *E. coli* cells and purified by using glutathione sepharose beads. KLHL3-Cullin3 complexes were immunoprecipitated from the lysates of HEK293T cells transiently expressing FLAG-Cullin3 and Halo-KLHL3. Then, the complexes were incubated in 20 μl of reaction buffer (50 mM Tris-HCl [pH 7.4], 2.5 mM MgCl2, 0.5 mM DTT, and 2 mM ATP) for 2 hr at 30°C with purified GST-WNK4-His (5 μg), 100 ng recombinant human E1 (Boston Biochem), 500 ng recombinant human UbcH5a/UBE2D1 (Boston Biochem), and 2.5 μg recombinant human ubiquitin (Boston Biochem). The reaction was terminated by the addition of SDS-PAGE sample buffer, followed by boiling for 5 min. The reaction mixtures were then subjected to immunoblot analyses with ubiquitin (Cell Signaling Technology) or His (Abcam) antibodies.

Quantitative RT-PCR

6.1441mmBoth kidneys were removed, immediately frozen in dry ice, and fragmented and homogenized in TRIzol Reagent (Invitrogen). Isolated total RNA was reverse-transcribed by using Omniscript reverse transcriptase (QIAGEN), and quantitative real-time PCR analysis was performed in triplicate by using SYBR Green I (Roche Applied Science) on LightCycler 2.0 (Roche). Amplification primers for *WNK4* were the same as reported previously (O'Reilly et al., 2006), and the primers for GAPDH were purchased from Roche Diagnostics. WNK4 mRNA levels were corrected by GAPDH mRNA levels.

Fluorescence Correlation Spectroscopy

Fluorescent TAMRA-labeled WNK4 peptides covering the PHAII mutation sites were prepared (Hokkaido System Science, Hokkaido, Japan). The sequence details of the peptides are shown in Figure 4. Human full-length KLHL3 was cloned into pGEX6P-1 vector. Recombinant GST fusion KLHL3 protein was expressed in BL21 *E. coli* cells and purified by using glutathione sepharose beads. The TAMRA-labeled WNK4 peptides were incubated at room temperature for 30 min with different concentrations of GST-KLHL3 (0–2 μM) in 1 × PBS with 0.05% Tween 20 reaction buffer, and the FCS measurements of single-molecule fluorescence were performed using the FluoroPoint-Light analytical system (Olympus) (Kuroki et al., 2007). The assay was performed in a 384-well plate. All experiments were performed in 10 s of data-acquisition time, and the measurements were repeated five times per sample.

Production of *Wnk4* BAC TG Mice

The BAC clone bMQ428o09, which contains the mouse genomic *Wnk4* locus, was used. For Southern blot analysis and PCR genotyping, a new *Spe*I site was created in intron 6 of the *Wnk4* genomic locus. The BAC modification was performed as previously described (Warming et al., 2005). Purified BAC DNA was then digested with *Swa*I, and the desired 36.8 kb fragment was isolated after fractionation via inverted pulse field gel electrophoresis, as reported previously (Lalioti et al., 2006). The purified fragment was injected into one-cell embryos of C57BL/6J mice. The copy number of the transgene was estimated by Southern blotting and quantitative PCR. The Animal Care and Use Committee of Tokyo Medical and Dental University approved this experiment (0120038B).

Blood Pressure Measurements

We measured blood pressure by using a radiotelemetric method (Mills et al., 2000) in which a blood pressure transducer (Data Sciences International, St. Paul, MN, USA) was inserted into the left carotid artery. Seven days after transplantation, each mouse was housed individually in a standard cage on a receiver under a 12 hr light-dark cycle. Systolic and diastolic blood pressure, heart rate, and activity were recorded every minute via radiotelemetry. Mice showed alternating periods of high activity (20:00–8:00) and low activity (8:00–20:00). For each mouse, we measured blood pressure values for more than 5 consecutive days and calculated the mean ± SEM of all values during both the high- and low-activity periods.

Blood Data Analyses

Blood for electrolyte analyses was obtained as described previously (Yang et al., 2007). Electrolyte levels were determined with an i-STAT analyzer (Fuso Pharmaceutical Industries, Osaka, Japan).

Statistical Analysis

Comparisons between the two groups were performed with unpaired t tests. ANOVA with Tukey's post hoc test was used to evaluate statistical significance in the comparison among multiple groups. p values <0.05 were considered statistically significant. Data are presented as the mean ± SEM.

SUPPLEMENTAL INFORMATION

Supplemental Information includes five figures and can be found with this article online at http://dx.doi.org/10.1016/j.celrep.2013.02.024.

LICENSING INFORMATION

ACKNOWLEDGMENTS

REFERENCES

Achard, J.M., Disse-Nicodeme, S., Fiquet-Kempf, B., and Jeunemaitre, X. (2001). Phenotypic and genetic heterogeneity of familial hyperkalaemic hypertension (Gordon syndrome). Clin. Exp. Pharmacol. Physiol. *28*, 1048–1052.

Ahlstrom, R., and Yu, A.S. (2009). Characterization of the kinase activity of a WNK4 protein complex. Am. J. Physiol. Renal Physiol. 297, F685–F692.

Bergaya, S., Faure, S., Baudrie, V., Rio, M., Escoubet, B., Bonnin, P., Henrion, D., Loirand, G., Achard, J.M., Jeunemaitre, X., and Hadchouel, J. (2011). WNK1 regulates vasoconstriction and blood pressure response to α 1-adrenergic stimulation in mice. Hypertension 58, 439–445.

Boyden, L.M., Choi, M., Choate, K.A., Nelson-Williams, C.J., Farhi, A., Toka, H.R., Tikhonova, I.R., Bjornson, R., Mane, S.M., Colussi, G., et al. (2012). Mutations in kelch-like 3 and cullin 3 cause hypertension and electrolyte abnormalities. Nature 482, 98–102.

Castañeda-Bueno, M., Cervantes-Pérez, L.G., Vázquez, N., Uribe, N., Kantesaria, S., Morla, L., Bobadilla, N.A., Doucet, A., Alessi, D.R., and Gamba, G. (2012). Activation of the renal Na+:Cl- cotransporter by angiotensin II is a WNK4-dependent process. Proc. Natl. Acad. Sci. USA 109, 7929–7934.

Chiga, M., Rai, T., Yang, S.S., Ohta, A., Takizawa, T., Sasaki, S., and Uchida, S. (2008). Dietary salt regulates the phosphorylation of OSR1/SPAK kinases and the sodium chloride cotransporter through aldosterone. Kidney Int. 74, 1403–1409.

Chiga, M., Rafiqi, F.H., Alessi, D.R., Sohara, E., Ohta, A., Rai, T., Sasaki, S., and Uchida, S. (2011). Phenotypes of pseudohypoaldosteronism type II caused by the WNK4 D561A missense mutation are dependent on the WNK-OSR1/SPAK kinase cascade. J. Cell Sci. 124, 1391–1395.

Cirak, S., von Deimling, F., Sachdev, S., Errington, W.J., Herrmann, R., Bönnemann, C., Brockmann, K., Hinderlich, S., Lindner, T.H., Steinbrecher, A., et al. (2010). Kelch-like homologue 9 mutation is associated with an early onset autosomal dominant distal myopathy. Brain 133, 2123–2135.

Duong Van Huyen, J.P., Bens, M., Teulon, J., and Vandewalle, A. (2001). Vasopressin-stimulated chloride transport in transimmortalized mouse cell lines derived from the distal convoluted tubule and cortical and inner medullary collecting ducts. Nephrol. Dial. Transplant. 16, 238–245.

Gamba, G. (2012). Regulation of the renal Na+-Cl- cotransporter by phosphorylation and ubiquitylation. Am. J. Physiol. Renal Physiol. 303, F1573–F1583.

Gordon, R.D. (1986). Syndrome of hypertension and hyperkalemia with normal glomerular filtration rate. Hypertension 8, 93–102.

Hoorn, E.J., Walsh, S.B., McCormick, J.A., Fürstenberg, A., Yang, C.L., Roeschel, T., Paliege, A., Howie, A.J., Conley, J., Bachmann, S., et al. (2011). The calcineurin inhibitor tacrolimus activates the renal sodium chloride cotransporter to cause hypertension. Nat. Med. 17, 1304–1309.

Kigoshi, Y., Tsuruta, F., and Chiba, T. (2011). Ubiquitin ligase activity of Cul3-KLHL7 protein is attenuated by autosomal dominant retinitis pigmentosa causative mutation. J. Biol. Chem. 286, 33613–33621.

Komers, R., Rogers, S., Oyama, T.T., Xu, B., Yang, C.L., McCormick, J., and Ellison, D.H. (2012). Enhanced phosphorylation of Na(+)-Cl- co-transporter in experimental metabolic syndrome: role of insulin. Clin. Sci. 123, 635–647.

Kuroki, K., Kobayashi, S., Shiroishi, M., Kajikawa, M., Okamoto, N., Kohda, D., and Maenaka, K. (2007). Detection of weak ligand interactions of leukocyte Ig-like receptor B1 by fluorescence correlation spectroscopy. J. Immunol. Methods 320, 172–176.

Lalioti, M.D., Zhang, J., Volkman, H.M., Kahle, K.T., Hoffmann, K.E., Toka, H.R., Nelson-Williams, C., Ellison, D.H., Flavell, R., Booth, C.J., et al. (2006). Wnk4 controls blood pressure and potassium homeostasis via regulation of mass and activity of the distal convoluted tubule. Nat. Genet. 38, 1124–1132.

Lee, Y.R., Yuan, W.C., Ho, H.C., Chen, C.H., Shih, H.M., and Chen, R.H. (2010). The Cullin 3 substrate adaptor KLHL20 mediates DAPK ubiquitination to control interferon responses. EMBO J. 29, 1748–1761.

Lin, M.Y., Lin, Y.M., Kao, T.C., Chuang, H.H., and Chen, R.H. (2011). PDZ-RhoGEF ubiquitination by Cullin3-KLHL20 controls neurotrophin-induced neurite outgrowth. J. Cell Biol. 193, 985–994.

Liu, Z., Xie, J., Wu, T., Truong, T., Auchus, R.J., and Huang, C.L. (2011). Down-regulation of NCC and NKCC2 cotransporters by kidney-specific WNK1 re-

vealed by gene disruption and transgenic mouse models. Hum. Mol. Genet. 20, 855–866.

Louis-Dit-Picard, H., Barc, J., Trujillano, D., Miserey-Lenkei, S., Bouatia-Naji, N., Pylypenko, O., Beaurain, G., Bonnefond, A., Sand, O., Simian, C., et al.; International Consortium for Blood Pressure (ICBP). (2012). KLHL3 mutations cause familial hyperkalemic hypertension by impairing ion transport in the distal nephron. Nat. Genet. 44, 456–460, S1–S3.

McCormick, J.A., and Ellison, D.H. (2011). The WNKs: atypical protein kinases with pleiotropic actions. Physiol. Rev. 91, 177–219.

McEvoy, J.D., Kossatz, U., Malek, N., and Singer, J.D. (2007). Constitutive turnover of cyclin E by Cul3 maintains quiescence. Mol. Cell. Biol. 27, 3651–3666.

Mills, P.A., Huetteman, D.A., Brockway, B.P., Zwiers, L.M., Gelsema, A.J., Schwartz, R.S., and Kramer, K. (2000). A new method for measurement of blood pressure, heart rate, and activity in the mouse by radiotelemetry. J. Appl. Physiol. 88, 1537–1544.

Moriguchi, T., Urushiyama, S., Hisamoto, N., Iemura, S., Uchida, S., Natsume, T., Matsumoto, K., and Shibuya, H. (2005). WNK1 regulates phosphorylation of cation-chloride-coupled cotransporters via the STE20-related kinases, SPAK and OSR1. J. Biol. Chem. 280, 42685–42693.

O'Reilly, M., Marshall, E., Macgillivray, T., Mittal, M., Xue, W., Kenyon, C.J., and Brown, R.W. (2006). Dietary electrolyte-driven responses in the renal WNK kinase pathway in vivo. J. Am. Soc. Nephrol. 17, 2402–2413.

Ohno, M., Uchida, K., Ohashi, T., Nitta, K., Ohta, A., Chiga, M., Sasaki, S., and Uchida, S. (2011). Immunolocalization of WNK4 in mouse kidney. Histochem. Cell Biol. 136, 25–35.

Ohta, A., Rai, T., Yui, N., Chiga, M., Yang, S.S., Lin, S.H., Sohara, E., Sasaki, S., and Uchida, S. (2009). Targeted disruption of the Wnk4 gene decreases phosphorylation of Na-Cl cotransporter, increases Na excretion and lowers blood pressure. Hum. Mol. Genet. 18, 3978–3986.

Oi, K., Sohara, E., Rai, T., Misawa, M., Chiga, M., Alessi, D.R., Sasaki, S., and Uchida, S. (2012). A minor role of WNK3 in regulating phosphorylation of renal NKCC2 and NCC co-transporters in vivo. Biol. Open 1, 120–127.

Rossier, B.C., and Schild, L. (2008). Epithelial sodium channel: mendelian versus essential hypertension. Hypertension 52, 595–600.

San-Cristobal, P., Pacheco-Alvarez, D., Richardson, C., Ring, A.M., Vazquez, N., Rafiqi, F.H., Chari, D., Kahle, K.T., Leng, Q., Bobadilla, N.A., et al. (2009). Angiotensin II signaling increases activity of the renal Na-Cl cotransporter through a WNK4-SPAK-dependent pathway. Proc. Natl. Acad. Sci. USA 106, 4384–4389.

Shimkets, R.A., Warnock, D.G., Bositis, C.M., Nelson-Williams, C., Hansson, J.H., Schambelan, M., Gill, J.R., Jr., Ulick, S., Milora, R.V., Findling, J.W., et al. (1994). Liddle's syndrome: heritable human hypertension caused by mutations in the beta subunit of the epithelial sodium channel. Cell 79, 407–414.

Sohara, E., Rai, T., Yang, S.S., Ohta, A., Naito, S., Chiga, M., Nomura, N., Lin, S.H., Vandewalle, A., Ohta, E., et al. (2011). Acute insulin stimulation induces phosphorylation of the Na-Cl cotransporter in cultured distal mpkDCT cells and mouse kidney. PLoS ONE 6, e24277.

Susa, K., Kita, S., Iwamoto, T., Yang, S.S., Lin, S.H., Ohta, A., Sohara, E., Rai, T., Sasaki, S., Alessi, D.R., and Uchida, S. (2012). Effect of heterozygous deletion of WNK1 on the WNK-OSR1/ SPAK-NCC/NKCC1/ NKCC2 signal cascade in the kidney and blood vessels. Clin. Exp. Nephrol. 16, 530–538.

Warming, S., Costantino, N., Court, D.L., Jenkins, N.A., and Copeland, N.G. (2005). Simple and highly efficient BAC recombineering using galK selection. Nucleic Acids Res. 33, e36.

Wilson, F.H., Disse-Nicodème, S., Choate, K.A., Ishikawa, K., Nelson-Williams, C., Desitter, I., Gunel, M., Milford, D.V., Lipkin, G.W., Achard, J.M., et al. (2001). Human hypertension caused by mutations in WNK kinases. Science 293, 1107–1112.

Wilson, F.H., Kahle, K.T., Sabath, E., Lalioti, M.D., Rapson, A.K., Hoover, R.S., Hebert, S.C., Gamba, G., and Lifton, R.P. (2003). Molecular